" Maturing the production standards of ultraporous structures for high density hydrogen storage bank operating on swinging temperatures and low compression" – MAST3RBoost

MAST3RBoost

D4.1 Report on literature and database gaps in MMCs & coatings for compressed H_2 & cryo-Temp.

Due date of submission: 31/01/2023

Actual submission date: 28/02/2023

Funded by the European Union

TABLE OF CONTENTS

Funded by the European Union. Views and opinions expressed are however those of the author(s) only and do not necessarily reflect those of the European Union or [name of the granting authority]. Neither the European Union nor the granting authority can be held responsible for them.

Funded by the European Union. Views and opinions expressed are however those of the author(s) only and do not necessarily reflect those of the European Union or [name of the granting authority]. Neither the European Union nor the granting authority can be held responsible for them.

PROJECT INFORMATION

Project full title: Maturing the production standards of ultraporous structures for high density hydrogen storage bank operating on swinging temperatures and low compression.

Acronym: MAST3RBoost

Call: HORIZON-CL4-2021-RESILIENCE-01

Topic: HORIZON-CL4-2021-RESILIENCE-01-17

Start date: 1st June 2022

Duration: 48 months

List of participants:

Number	Name of beneficiary	Acronym of beneficiary	Country
1	ENVIROHEMP	ENV	Spain
2	CONTACTICA	CTA	SPAIN
3	Consejo Superior de Investigaciones Científicas	CSIC	Spain
4	Spike Renewables Srl	SPIKE	Italy
5	EDAG Engineering GmbH	EDAG	Germany
6	Nanolayers	NANO	Estonia
7	FUNDACIÓN CIDETEC	CIDETEC	Spain
8	Leichtmetallkompetenzzentrum Ranshofen GmbH	LKR	Austria
9	University of Pretoria	UP	South Africa
10	Council for Scientific and Industrial Research	CSIR	South Africa
11	PSA	PSA	Portugal
12	TWI Ltd	TWI	UK
13	University of Nottingham	UoN	UK

Funded by the European Union. Views and opinions expressed are however those of the author(s) only and do not necessarily reflect those of the European Union or [name of the granting authority]. Neither the European Union nor the granting authority can be held responsible for them.

DELIVERABLE DETAILS

Document Number:	D4.1
Document Title:	Report on literature and database gaps in MMCs & coatings for compressed H2 & cryo-Temp.
Dissemination level	PU – Public
Period:	PR1
WP:	WP4 – "Development and testing of advanced, fibre-reinforced lightweight metal alloys and coatings for hydrogen storage vessel"
Task:	4.1 – "Development of a catalogue of lightweight metal alloys and preliminary testing of sample specimens based on waDED state-of-the-art".
Author:	cidetec surface engineering FUNDACIÓN CIDETEC
Contributors:	AIT AUSTRIAN INSTITUTE OF TECHNOLOGY Leichtmetallkompetenzzentrum Ranshofen GmbH (LKR)
	TWI TWI Ltd (TWI)
Abstract:	This deliverable includes a literature review to develop a catalogue of lightweight metal alloys based on waDED state-of-the-art. This literature review will help to determine the state-of-the-art in terms of lightweight metal alloy properties, the available standards for testing of thermo-physical & mechanical analysis under H_2 and the catalogue of suitable protective coatings to act as a H_2 barrier at cryogenic tempreatuers.

Funded by the European Union. Views and opinions expressed are however those of the author(s) only and do not necessarily reflect those of the European Union or [name of the granting authority]. Neither the European Union nor the granting authority can be held responsible for them.

1 INTRODUCTION

This document contains the deliverable 4.1 associated with the Task 4.1 "Development of a catalogue of lightweight metal alloys and preliminary testing of sample specimens based on waDED state-of-the-art" [M1-M18] and the WP4 "Development and testing of advanced, fibre-reinforced lightweight metal alloys and coatings for hydrogen storage vessel" [M1-M36].

The document includes a compilation of literature reviews of hydrogen embrittlement (HE) of lightweight metal alloys/MMC, waDED alloys for hydrogen cryogenic applications, coatings, and prevention of HE as well as hydrogen testing methodologies.

2 LITERATURE REVIEW

2.1 INTRODUCTION

The exposure of metallic alloys to a hydrogen-bearing environment is known to compromise the performance of alloys[1]. The extent of damage varies from one alloy to the other depending on multiple factors such as the crystal structure, hydrogen transport properties, mechanical properties and extent of hydrogen uptake. For wrought alloys this has been investigated for many years in order to understand the interactions of the different factors[2]. The advent of additive manufacturing (AM) has introduced new classes of alloys with distinct microstructural properties that have different responses to in-service environments to the well-studied wrought materials. Extensive hydrogen embrittlement studies on AM alloys are still lagging behind compared to wrought processes, not least due to the time that has been. This poses a limitation on the use of new AM alloys in hydrogen environments, which is crucial for the development of the upcoming hydrogen economy.

There are many different variants of additive manufacturing processes such as Direct Energy Deposition (DED) and Powder Bed Fusion (PBF), both applied by the use of either laser, arc or electron beam heat sources. Wire Arc Additive Manufacturing (WAAM) is a DED process that utilises a wire feed that is deposited on a substrate by an arc source. The WAAM process benefits from the advantage of having high deposition rates compared to other AM process thus allowing fast build turnaround while achieving high dimensional control of the final product.

This literature review evaluates the available literature on hydrogen embrittlement (HE) of three classes of light alloys, namely; aluminium, magnesium and fibre reinforced aluminium matrix alloys.

2.2 SOURCES OF HYDROGEN IN METALLIC ALLOYS

There are a number of ways HE can be manifested in metallic alloys. Internal hydrogen (IH) embrittlement can occur by having pre-existing hydrogen in the microstructure while being under sustained loading leading to sub-critical cracking. IH can be introduced from conventional wrought manufacturing or AM processes[3]. IH embrittlement has been known to affect alloys with high hydrogen solid solution solubility such as Ti based alloys[4]. Aluminium and Magnesium exhibit very little adverse reaction, if any, to IH embrittlement due to low solid solution solubility of hydrogen in the microstructure. The main sources of IH can come from surface cleaning operations such as acid pickling or heat treatment in hydrogen bearing environments in steels. Additionally, welding or AM operations conducted on a contaminated working piece, in combination with moisture pick up from feedstock (wire or powder) or shielding gas can introduce hydrogen into a fabricated product[56]. IH embrittlement is out of scope of this review document since light alloys are relatively innocuous to this kind of HE. However, it is important to recognize that the introduction of hydrogen (IH) from welding and additive manufacturing (AM) processes can result in hydrogen gas porosity, which can adversely affect

Funded by the European Union. Views and opinions expressed are however those of the author(s) only and do not necessarily reflect those of the European Union or [name of the granting authority]. Neither the European Union nor the granting authority can be held responsible for them.

the mechanical properties of an alloy but may not necessarily cause embrittlement. Nevertheless, aluminium alloys are particularly susceptible to this issue, as they commonly suffer from hydrogen gas porosity during fabrication due to the low solid solution solubility of hydrogen in the aluminium microstructure[7].

Hydrogen environment embrittlement (HEE) involves sub-critical cracking of alloys under sustained loads while simultaneously being exposed to a hydrogen bearing environment. This affects many metallic alloys, including steel (ferritic and austenitic), aluminium, titanium and nickel alloys[1]. One of the main sources of hydrogen leading to HEE comes from what is termed a Redox reaction, either via electrochemical processes such as cathodic protection or environmental corrosion processes in electrolyte solutions or even moist environments [4, 89]. Recent research on environmental assisted cracking (EAC) of aluminium aerospace alloys have shown that thick plate 7xxx series alloys can be susceptible to hydrogen assisted EAC in moist environments even at relative humidity levels as low as 20%[8].

The other source of hydrogen is exposure to high-pressure gaseous (molecular) and liquid hydrogen commonly found in the space industry and more recently in the hydrogen economy. The ambition to replace fossil fuels with hydrogen energy source is expected to increase the scope of materials being exposed to gaseous hydrogen at cryogenic conditions when considering applications for hydrogen production, hydrogen-storage, and hydrogen transportation[1].

This review will therefore focus, albeit not exclusively, on gaseous HE of light alloys, but also on the adverse effects of hydrogen on the performance of light alloys when exposed to gaseous hydrogen, in particular in relation to AM processes. Additionally, some cases of H-assisted EAC in benign environments such as humid air may be discussed to illustrate hydrogen failure modes.

2.3 HYDROGEN UPTAKE AT THE METAL SURFACE

Hydrogen uptake in metallic alloys occurs through a sequence of adsorption and absorption processes of both diatomic and monoatomic hydrogen on the metal surface. Upon exposure to H_2 gas, the diatomic hydrogen molecules are physically adsorbed onto the surface by weak Van der Waals forces. Subsequently, the diatomic hydrogen molecules dissociate into monoatomic hydrogen at the surface through chemisorption processes i.e. formation of covalent bonded on the surface (eq.1)[7].

$$H_{2(g)} \leftrightarrow H_{2(p)} \leftrightarrow 2H_{(c)} \dots [1]$$

The chemisorbed monoatomic hydrogen can then be absorbed into metal substrate (eq.2) or recombine with another hydrogen atom to form again an H_2 molecule and escape the surface. The hydrogen recombination reaction could also occur by an electrochemical process route (eq.3-4)[10].

$$H_{(c)} \rightarrow H_{(abs)} \dots [2]$$

$$H_{(c)} + H_{(c)} \rightarrow H_{2(p)} \rightarrow H_{2(g)} \dots [3]$$

$$H_{(c)} + H^{+1} + e^{-1} \rightarrow H_{2(g)} \dots [4]$$

Apart from the direct decomposition of hydrogen gas, monoatomic hydrogen can be produced on a metal surface via electrochemical processes. The electrochemical processes include the direct reduction of water molecules (eq.5) or reduction of H+ ions (eq.6) resulting from corrosion reactions or impressed cathodic currents (cathodic protection) which produces monoatomic hydrogen on the surface which can then be absorbed into the material[1].

Funded by the European Union. Views and opinions expressed are however those of the author(s) only and do not necessarily reflect those of the European Union or [name of the granting authority]. Neither the European Union nor the granting authority can be held responsible for them.

$$H_2O \rightarrow OH^{-1} + H^{+1} + e^{-1} \leftrightarrow \frac{1}{2}H_2 \rightarrow OH^{-1} \dots [5]$$
$$H^{+1} + e^{-1} \leftrightarrow H_c \dots [6]$$

A summary of the chemical and electrochemical reactions involved in hydrogen uptake of metals are summarised in the schematic diagram in Figure 1.

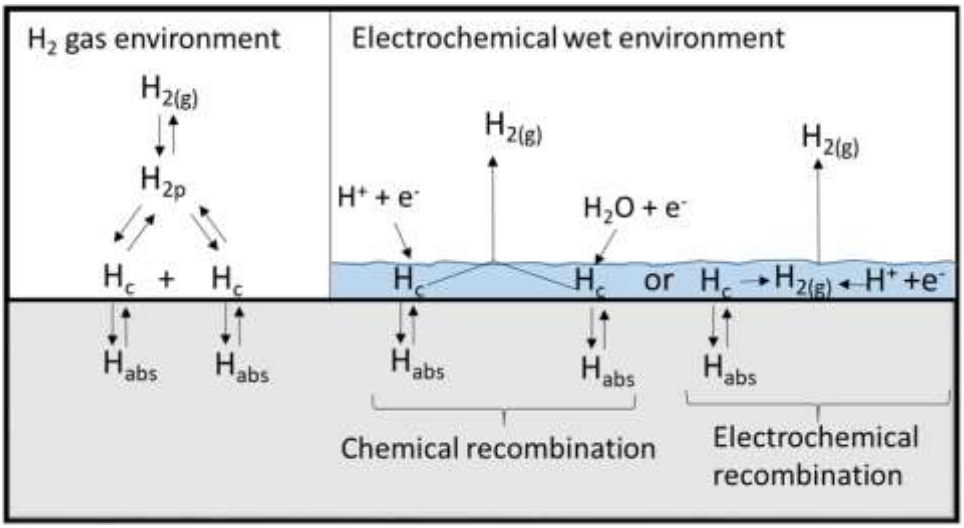

Figure 1. Schematic illustration of hydrogen adsorption and absorption processes in dry H_2 gas environments (left) and in wet environments (Right). c: chemisorption, p: physisorption.

3 HYDROGEN EMBRITTLEMENT OF ALUMINIUM ALLOYS

3.1 HYDROGEN UPTAKE PROPERTIES

Unlike most ferrous and non-ferrous metals with BCC, FCC and HCP crystal structures; aluminium alloys do not suffer from HE in dry hydrogen gas at ambient temperatures[11, 12]. This characteristic feature of aluminium alloys is attributed to the coherent oxide layer of aluminium oxide (Al_2O_3) that covers the exposed surfaces. The tenacious Al_2O_3 layer that forms on aluminium surface provides a high energy barrier to the chemisorbed dissociation process of the adsorbed H_2 molecules into monoatomic hydrogen thus limiting hydrogen uptake in dry hydrogen gas environments[7]. This material specific behaviour had been tested in practice by conducting sustained load tensile tests in high pressure dry hydrogen gas environments at ambient conditions[11]. Tensile strength and ductility of AA 6061-T6 and AA 7075-T73 did not show any reduction when tested in hydrogen gas up to 10,000 psi (~690 bar) pressure compared to the reference tests in helium. Additionally, Lorenz et al.[13] found no changes to the threshold stress intensity factor (KTH) of surface flawed tension specimens of AA2219-T6 tested under sustained load conditions in 5200 psi (358 bar) H_2 gas. The measured Kth was 30.8 MPa.m1/2 for 0.75" and 1.00" plates. Similar testing was done on AA2219-T6 weldments were found to yield a Kth value of 28.6 MPa.m1/2. Both Kth values were found to be very close to the expected fracture toughness KIC values for the alloy around 35 MPa.m1/2[13].

During 1970s Speidel and Hayatt conducted a similar experiment, but on high strength 7xxx series alloys, where they bolt loaded (constant displacement) a double cantilever beam (DCB) specimen near to KIC in dry hydrogen environment (0.01% Rh and 1 bar 100% H_2 gas) for 47 days. The DCB specimen did not exhibit any crack growth within the prolonged period of testing until after humidity was introduced (100% Rh) and crack growth was observed[12]. The crack propagation rates measured in moist hydrogen varied from one copper rich grade to another copper lean grade, in agreement with the general trends observed in EAC/SSC testing in moist

Funded by the European Union. Views and opinions expressed are however those of the author(s) only and do not necessarily reflect those of the European Union or [name of the granting authority]. Neither the European Union nor the granting authority can be held responsible for them.

and saline environments [9, 14 15]. Therefore, dry hydrogen gas is largely ineffective on aluminium alloys unless an aqueous environment can be present.

Most cases of hydrogen embrittlement in aluminium alloys reported in the literature involve exposure to aqueous environments of varying severity to study hydrogen-assisted cracking. The process of hydrogen uptake usually involves a series of electrochemical (corrosion) reactions that produce localised hydrogen and subsequent absorption, usually at crack tips, causing embrittlement. Cathodic impressed currents have been utilised in numerous studies to introduce hydrogen into aluminium alloys[16]. However, there are limited to no applications under cathodic protection, as aluminium alloys can corrode under a specific cathodic overpotential window. Additionally, hydrogen can also be introduced during the fabrication of components using additive manufacturing (AM) techniques, such as Laser Powder Bed Fusion (L-PBF), as reported by McFalls, or during welding operations [36].

3.2 HYDROGEN SOLUBILITY AND DIFFUSIVITY IN ALUMINIUM ALLOYS

Aluminium has low solubility and diffusivity for hydrogen in the solid phase, which can lead to hydrogen effects being overlooked. Other materials with face-centered cubic (FCC) structures are typically less susceptible to hydrogen embrittlement than metals with BCC and HCP crystal structures. The solubility of hydrogen in pure aluminium varies in the literature, with values around 1.5x10-12 atomic fraction[17]. Alloying elements such as Li, Mg, Cu, Si, and Zn can increase hydrogen solubility, and lattice vacancies, dislocations, grain boundaries, and voids can trap hydrogen ANY[18]. Thus, the presence of additional trapping sites in aluminium alloys increase the total capacity to hold hydrogen than in pure aluminium. Generally, the hydrogen solid solubility in aluminium is low. However, in the liquid phase, the solubility of hydrogen is much higher, at around $1x10^{-6}$ atomic fraction [17], so care must be taken during cooling molten aluminium to prevent porosity, especially during welding. Trapping sites such as voids can also serve as nucleation sites for hydrogen gas bubble precipitation if the aluminium is supersaturated with hydrogen[19].

The diffusivity of hydrogen within solid aluminium is also slow, with a typical diffusivity of approximately 2.5x10-14 m2s-1 (2.5x10-10 cm2s-1) at room temperature for pure aluminium[7]. However, the values reported in the literature vary widely due to factors such as differences in measurement methods, the low volumes of gas involved, and the presence of lattice defects that can affect measurement accuracy. For instance, Talbot and Anyalebechi reported diffusivity values ranging from about 10-13 to 10-14 m2s-1 (10-9 to 10-10 cm2s-1) at room temperature, whereas at 500 °C, the value was around 10-8 m2s-1[20, 21]. Some experts have suggested that the movement of dislocations may facilitate faster diffusion of hydrogen[19], but there is no direct evidence to support this idea[7].

The diffusivity of hydrogen in aluminium is strongly influenced by alloying and microstructure. According to studies[20 7] alloying with Mg and Li significantly reduces diffusivity compared to pure aluminium. In addition, lattice defects such as porosity can act as trapping sites, thereby reducing diffusivity. Young and Scully have identified three distinct types of trapping sites: interstitial lattice sites, dislocations, and vacancies[7]. These sites are important in assessing the performance of AM materials because they decrease the amount of hydrogen available to cause embrittlement in materials.

3.3 HYDROGEN INDUCED CRACKING IN ALUMINIUM ALLOYS

Due to the limited effectiveness of dry hydrogen absorption in aluminium, most available data in the literature on the effects of hydrogen exposure on mechanical properties of aluminium alloys are derived from electrochemically charged or environmental exposure of samples, which may not accurately represent the

Funded by the European Union. Views and opinions expressed are however those of the author(s) only and do not necessarily reflect those of the European Union or [name of the granting authority]. Neither the European Union nor the granting authority can be held responsible for them.

response to gaseous hydrogen exposure. Nonetheless, these studies demonstrate the impact of increasing hydrogen concentration on the mechanical properties of aluminium alloys.

Studies have consistently reported a negative effect of hydrogen charging on the tensile properties of aluminium alloy samples. For instance, Watson et al. investigated the impact of hydrogen charging on the mechanical properties of pure aluminium and found a 15% change in elongation [19]. Despite hydrogen-charged samples showing a ductile failure mode, there was a substantial reduction in the measured ductility. Increased dislocation density and surface microhardness were observed through transmission electron microscopy (TEM) after hydrogen charging. Micro-hardness measurements indicated that recovery occurred in two stages during subsequent annealing. The first stage was attributed to cold work recovery (i.e., dislocation annihilation), and the second stage was attributed to hydrogen diffusion from close to the surface into the bulk of the metal.

Holroyd et. al (1981) reported strain rate dependent behaviour in the tensile properties of aluminium alloys tested under environmental exposure, with a greater drop in performance observed at lower strain rates (10-6 s-1) compared to a strain rate of 10-5 s-1 [22]. This behaviour suggests that hydrogen diffusion plays a significant role in determining the mechanical response of the material. The effect of the strain rate EAC properties was reported in a more recent study on 3rd generation 7xxx series alloys. SSRT testing was conducted in humid environments at 10-6 and 10-7 s-1 nominal strain rates. The results had shown that some alloys that are susceptible to EAC exhibited a 300% reduction in the plastic elongation failure when tested at 10-7 s-1[8].

Numerous studies have investigated the environmentally assisted cracking (EAC) behaviour of aluminium alloys, with a particular focus on solid solution strengthened high magnesium 5xxx series alloys (e.g., 5083) in the sensitized condition and precipitation hardened 7xxx series alloys containing Zn and Mg alloy composition [14, 15 8,9,23]. The failure mechanism in such alloys has been attributed to EAC, resulting in typical intergranular and transgranular fracture surfaces similar to those observed in hydrogen embrittlement of other metallic alloys[4]. The observed changes in elongation values in response to hydrogen exposure suggests that small levels of hydrogen can cause embrittlement. However, there is no general consensus across the literature regarding the effect of hydrogen on yield strength and ultimate tensile strength (UTS), although any reported changes tend to be small.

4 HYDROGEN EMBRITTLEMENT OF MAGNESIUM ALLOYS

Magnesium alloys, like aluminium alloys, are vulnerable to Stress Corrosion Cracking (SCC) even in benign environments such as distilled water. This susceptibility is primarily attributed to the high corrosion rates and electrode potential of pure magnesium and magnesium alloys compared to other metals and alloys in stress-free conditions. Although the exact mechanism of SCC in magnesium alloys is a topic of ongoing debate, there is convincing evidence supporting hydrogen-assisted crack propagation in combination with other anodic-based corrosion mechanisms. The exact nature of the metal-hydrogen interaction that results in embrittlement is still not well understood.

In addition to the possible hydrogen-based mechanisms such as decohesion, enhanced plasticity, and dislocation emission models, magnesium alloys are also prone to forming magnesium-hydrides when exposed to pure hydrogen environments. This can lead to further embrittlement and cracking of the material[24].

4.1 FORMATION OF MAGNESIUM HYDRIDES

The formation of stable hydride phases is a significant factor affecting the performance of Hexagonal Close Packed (HCP) alloys such as zirconium and titanium. The subsequent fracture of these hydride phases can have a major impact on the material's behaviour under certain conditions[24, 25]. Magnesium and its alloys have

Funded by the European Union. Views and opinions expressed are however those of the author(s) only and do not necessarily reflect those of the European Union or [name of the granting authority]. Neither the European Union nor the granting authority can be held responsible for them.

a hexagonal close-packed atomic structure, which can form hydrides (MgH2) with a tetragonal structure. However, the hydrides that form in magnesium alloys are less stable compared to those formed in zirconium and titanium alloys. This is because the magnesium hydride decomposes at temperatures above 287 °C under 1 bar H2 partial pressure[26]. The dissociation temperature will vary depending on the H2 partial pressure in the environment. For example, the dissociation temperature of MgH2 at 30 and 100 bar H-2 partial pressures are at around 427 °C and 450 °C[26,27].

4.2 HYDROGEN DIFFUSION AND SOLUBILITY IN MAGNESIUM

Hydrogen can be present in magnesium alloys in octahedral sites of the HCP crystal lattice[27]. However, measuring hydrogen diffusion and solubility in magnesium and its alloys can be challenging due to various factors. For instance, the formation of MgH2 near the surface exposed to hydrogen can limit hydrogen transport kinetics because of its extremely low diffusion coefficient (order of 10-16 m2/s at 25 ºC). Additionally, the formation of tenacious layers of Mg(OH)2 and MgO can also restrict hydrogen uptake. As a result, literature on hydrogen diffusion (DH) in magnesium alloys is limited.

For example, Knotec et al. reported a DH - of 6.7 × 10−13 m2/s in pure Mg[24], while Nishimura and other researchers estimated a DH of 10−9 m2/s in pure Mg by extrapolating from high-temperature gas permeation measurements (~200 ºC) [28, 29]. The presence of alloying elements (such as Al) is expected to reduce the DH due to the additional reversible trapping sites. Dietzel et al. reported an effective DH for magnesium alloy AZ91 of 2.0 × 10−13 m2/s based on modelling hydrogen assisted failure from mechanical tests[30].

It can be challenging to determine the exact DH values of pure Mg due to experimental complexities associated with each method. However, for hydrogen gas storage applications, it may be more suitable to consider the extrapolated upper range of values, which is between 10-10-10-9 m2/s extrapolated from hot gas permeation when considering hydrogen gas storage applications. As a reference, those values are close to lattice diffusion coefficient of ferritic steels that yield DH values between 10-10 – 10-8 m2/s[31, 32].

San Martin and Manchester [33] found that the dependency of hydrogen solubility (at.%) with temperature at 1 bar H2 partial pressure was given by:

$$S(\text{at\%}) = 0.0023 + 1.28.\exp\left(\frac{22{,}780}{\text{R.T}}\right) \ldots [1]$$

$$\text{R} - \text{gas contant, T} - \text{temperature in K}$$

At high temperatures close to the melting point (~600 ºC), the hydrogen solubility values reported in the literature for pure magnesium were approximately 0.06-0.07 at. % (25-27 ppm). Extrapolation of these values to room temperature yields a hydrogen solubility of 0.002 at. % (0.08 ppm) in pure magnesium[33]. Other researchers have found that the hydrogen solubility in Mg follows Sievert's law, which states that the hydrogen solubility in the lattice is proportional to the square root of H2 partial pressure[34, 35]. The hydrogen solubility relationships suggested by the authors in ref [33,3435] were based on results from high temperature experiments that excludes the effects of magnesium hydrides as they dissociate above 287 °C, which leads higher values. This may be the reason why there is limited information on the solubility limit or the maximum hydrogen concentration in magnesium at room temperature in the literature. However, it should be noted that conducting high-temperature hydrogen diffusion and solubility experiments on magnesium alloys can be extremely difficult due to its high vapour pressure at high temperatures and chemical reactivity. Thus, discrepancies between the data available in the literature are to be expected.

Funded by the European Union. Views and opinions expressed are however those of the author(s) only and do not necessarily reflect those of the European Union or [name of the granting authority]. Neither the European Union nor the granting authority can be held responsible for them.

4.3 EVIDENCE SUPPORTING HYDROGEN INDUCED CRAKING IN MAGNESIUM ALLOYS

Several studies have reported both IH and HE embrittlement of magnesium alloys[29,30,36, 37] Magnesium alloys can be hydrogen charged by chemical or electrochemical processes, such as exposure to distilled water or cathodic protection. However, unlike in aluminium alloys, hydrogen may also be introduced into magnesium alloys by exposure to high-pressure hydrogen gas environments. In the context of studying metal-hydrogen interactions, gas charging may be a more appropriate method since it avoids contributions from general or local corrosion processes that are prevalent in high-reactivity metals such as Mg and Al. This is because gas charging involves exposing the sample to a controlled hydrogen environment, where the hydrogen pressure and temperature can be varied to study the effect of these parameters on hydrogen uptake and its effect on the mechanical properties of the material. Additionally, gas charging is a non-destructive method and does not introduce any foreign ions into the sample, making it suitable for studying the fundamental mechanisms of hydrogen embrittlement in magnesium alloys.

Winzer et al. investigated the effects of hydrogen on a Mg-Al alloy (AZ91) through exposure to both hydrogen gas and distilled water environments [36,37]. The authors pre-charged AZ91 in 3 MPa hydrogen gas at 300 °C for 14 hours to achieve saturation, and then immediately subjected the sample to slow strain rate testing (10-4 s-1) in air. The measured hydrogen content after pre-charging ranged between 6.9x10-2 – 1.9x10-1 at.% [28], with some contribution from surface oxides. The pre-charged samples exhibited significant reduction in elongation and failed below the yield stress, whereas control specimens tested under the same conditions in air without hydrogen pre-charging failed with appreciable plastic deformation[36]. The hydrogen pre-charged specimens showed an 80% decrease in plastic strain and 50% reduction in tensile strength compared to the control specimens. The HE damage inflicted by the H2 gas pre-charging and subsequent fast fracture (10-4 s-1) was more severe than SCC testing in distilled water at a strain rate range of 1-5 -10-7 s-1. The authors attributed the hydrogen pre-charging test failures to hydride embrittlement, as evidenced by the quasi-porous features observed on the fracture surface. However, the process of hydride formation at the crack tip under high strain rate conditions is not well understood, unless the hydrides would in fact pre-exist in the microstructure just after hydrogen pre-charging and then decompose post failure acting as a metastable phase. On the other hand, the mechanism of failure of magnesium alloys in distilled water tests are often attributed to SCC with a fracture appearance typical of SCC cleavage fracture, in addition to a characteristic HCP “flute” fracture surface akin to reports from Lynch and others[4,36,38]. Those fracture surface features were not observed in the hydrogen pre-charged samples indicating a different failure mechanism.

4.4 FIBER REINFORCED AL MATRIX ALLOYS FOR HYDROGEN APPLICATIONS

Fibre reinforced Al matrix alloys are part of the group Al-metal matrix composites (MMCs). MMCs are composed of a minimum of two chemically and physically different phases that are dispersed in such a way that they provide qualities that are not possible with/or from either of the phases alone[39].

4.4.1 Metal Matrix Composites

These materials offer a wide array of advantages compared to unreinforced metals. In the case of carbon fibre reinforced metals, the composites possess higher dimensional stability, improved cyclic fatigue resistance and weight saving potential due to the relatively low density of carbon. In comparison with conventional polymer matrix composites, MMCs offer a higher temperature range in which they can be used as well as higher electrical and thermal conductivity and higher resistance to radiation. Ou et al.[40] have researched the influence of changes in the temperature on the mechanical properties of carbon fibre reinforced polymer (CFRP) materials. A decrease in temperature below 25°C result in embrittlement of the resin matrix. This makes CFRP

Funded by the European Union. Views and opinions expressed are however those of the author(s) only and do not necessarily reflect those of the European Union or [name of the granting authority]. Neither the European Union nor the granting authority can be held responsible for them.

a bad fit for the application in the MAST3RBoost project, which operates in a temperature range of -196 °C to -140 °C.

Composites can either be classified based on their matrix material or on the shape of the reinforcement used. The different reinforcement classes are continuous fibre reinforced composites, discontinuous reinforced composites and particulate reinforced composites[41] as shown in Figure 2.

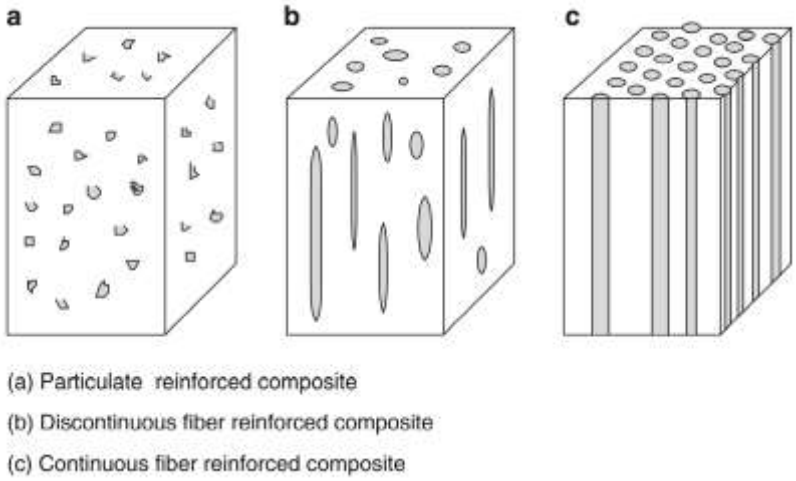

Figure 2. Classification of composites by reinforcement shape [41]

The focus in this project is on the manufacturing of continuous fibre reinforced composites. Continuous fibres offer the highest mechanical properties out of the reinforcement shapes, due to their direct reinforcement in the direction of the greatest occurring load. The strength perpendicular to the fibre direction is very small in comparison and mainly depends on the matrix material and the fibre matrix interface. The main drawback of continuous fibre reinforced MMCs is the high cost and labour intense production.

4.4.2 Manufacturing methods

There are many different production methods, which can be used to manufacture MMCs. The choice of what process to use depends on many factors, the most important of which are the shape of reinforcement, the preservation of the reinforcement's strength, the minimization of the damage to the reinforcement and promotion of the wetting and bonding between the two constituents[42]. These procedures, for the most part, include liquid and solid processing. Some procedures may use a variety of deposition techniques or an approach that includes a reinforcing phase[43]. The incorporation of the fibres via the waDED process would be in this group of manufacturing methods. The process under these circumstances is a novelty and therefore is not mentioned or further elaborated in any of the available literature.

Funded by the European Union. Views and opinions expressed are however those of the author(s) only and do not necessarily reflect those of the European Union or [name of the granting authority]. Neither the European Union nor the granting authority can be held responsible for them.

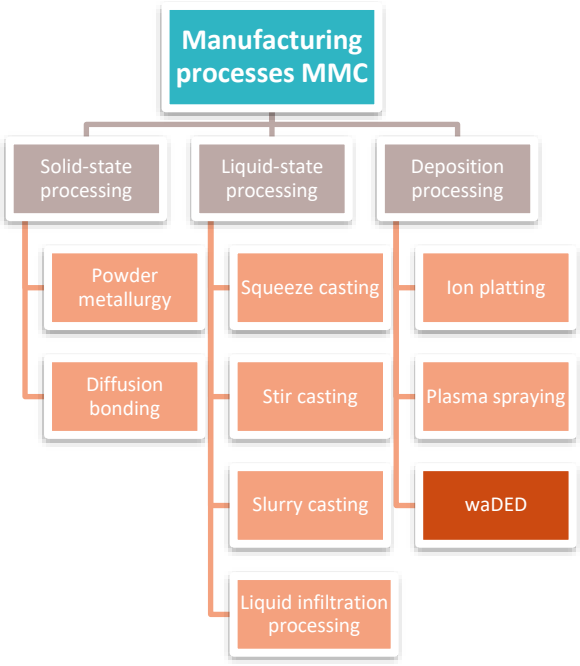

Figure 3. Adapted overview MMC manufacturing options [44]

4.4.3 Matrix materials

The end performance of a metal matrix composite is determined by three critical factors: the matrix, the reinforcement, and the interface between matrix and reinforcement[45].

The most commonly used metals are aluminium, magnesium, and titanium. These materials are characterized by their low density and high specific strength and are commonly used in the automotive and aerospace fields. The researchers at LKR have done some work on the manufacturing of continuous fibre reinforced aluminium with liquid infiltration processing. The biggest issue in the manufacturing of CF-Al-MMC via liquid-state infiltration is the formation of unwanted phases at the fibre matrix interphase. The formation of aluminium carbides during the infiltration reduces the mechanical properties of the carbon fibres. The addition of magnesium to the aluminium alloy has proven to reduce the formation of Al_4C_3 brittle phase[46].

4.4.4 Reinforcements

Reinforcements for MMCs need to have high strength, high elastic modulus, low thermal expansion coefficient and a high melting point or decomposition temperature. The most researched materials in this matter are aluminium oxides (Al_2O_3), carbon fibres, ceramics, and ceramic fibres[41]. As shown in Figure 2 the reinforcements for MMCs come in different shapes. The main distinguishment between the three groups is their aspect ratio of diameter to length. Depending on the type of reinforcement a fitting manufacturing method has to be chosen. LKR focuses on MMCs with continuous fibre reinforcement in their work.

4.4.5 MMC pressure vessel

MMCs are usually not the first choice of material for the manufacturing of pressure vessels. The technology has yet to be matured to a point where applications such as a pressure vessel can be done in an economically efficient manner. Compared to polymer matrix composites (PMC), MMC have better fire resistance, a wider temperature range and no risk of outgassing[47].

Several projects in producing pressure vessels with MMCs have been conducted. In 2005 Touchstone Research

Funded by the European Union. Views and opinions expressed are however those of the author(s) only and do not necessarily reflect those of the European Union or [name of the granting authority]. Neither the European Union nor the granting authority can be held responsible for them.

Laboratory, Ltd. Manufactured a cylindrical pressure vessel made from Al_2O_3 fibre reinforced 99,99% pure aluminium. This was done by pre impregnating the fibres with the molten aluminium matrix and utilising the filament winding technology, which has been used in the manufacturing of traditional PMC components[47,48].

Figure 4: Open ended wet filament wound AMC cylinders as produced by MetPreg [47]

These demonstrators (Figure 4) have then been tested in pressure test rig. The setup restricted the axial movement of the tube so that only hoop stresses could be measured. This is shown in Figure 5. This vessel withstood an internal pressure of 23 MPa with a wall thickness of 1,85mm and an inner diameter of 101mm.

Figure 5: Pressure test fixture AMC demonstrator [47]

In 2019 the researchers at TISICS Ltd. manufactured a pressure vessel made from SiC fibre reinforced titanium matrix. Their tube was produced using the hot isostatic pressing process. This process is part of the diffusion bonding group. A stack of alternating layers of aligned fibres and foil are placed in a steel tool. The stack is then exposed to high pressure and temperature to consolidate the individual layers into a composite. In the case of TISICS the process parameters are 950°C and 50-100MPa[49]. This way they produced multiple tubes made out of the MMC material with varying layups. These tubes were then pressure tested and the strains in the material were measured, Figure 6. The highest achieved pressure in this vessel was 280 bar at a wall thickness of 1,858 mm.

Funded by the European Union. Views and opinions expressed are however those of the author(s) only and do not necessarily reflect those of the European Union or [name of the granting authority]. Neither the European Union nor the granting authority can be held responsible for them.

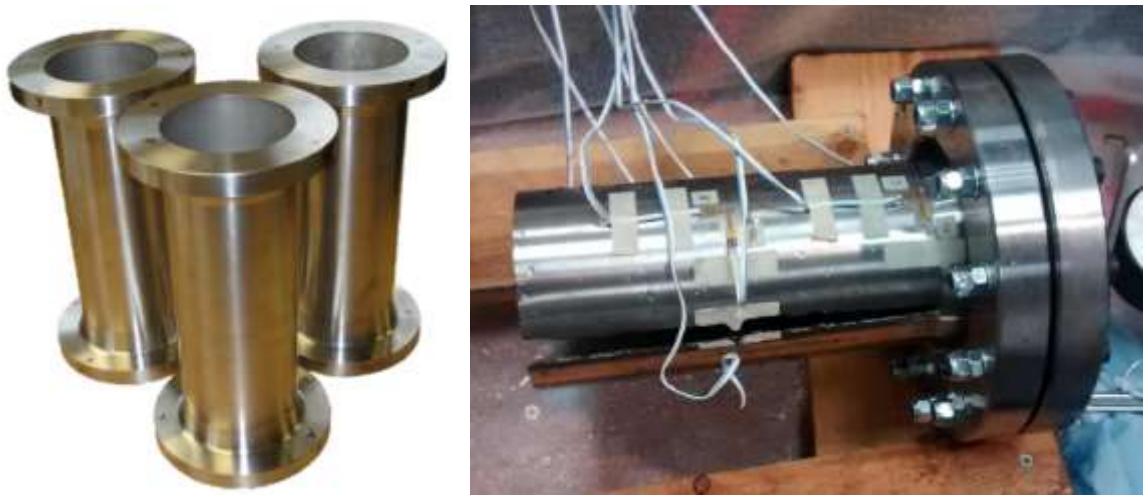

Figure 6: TISICS MMC pressure tube, left) pretesting pressure tubes, right) pressure tube after failure [49]

4.5 waDED ALLOYS FOR HYDROGEN CRYOGENIC APPLICATIONS

Additive manufacturing (AM) technologies have been the focus of many research programs in the recent years. They offer a lot of advantages to conventional, already established processes. Especially in the early stages of development of new products or structures, here the costs of manufacturing can be minimised by utilising the potential AM-technologies offer. The number of different AM-technologies on the market increased significantly over the last decades. One of them is wire-arc additive manufacturing (waDED).

4.5.1 Microstructure evolution of waDED

4.5.1.1 Aluminium

Higher thermal exposure in aluminium alloys often leads to grain coarsening and challenging control of second phases[50,51]. The microstructures highly depend on the location of the deposited layer. Each layer experiences different heating and cooling during processing as well as intrinsic heat treatment (IHT)[51]. Generally speaking, the higher layers exhibit a finer structure due to a smaller heat input of subsequent layers than layers at the bottom. In the case of Wu et. al[50], they observed an average spacing of secondary dendrite arms of about 4µm at the upper regions of their 4043 Al-alloy and about 8µm in the lower regions. This difference in microstructure can be seen in Figure 7.

Funded by the European Union. Views and opinions expressed are however those of the author(s) only and do not necessarily reflect those of the European Union or [name of the granting authority]. Neither the European Union nor the granting authority can be held responsible for them.

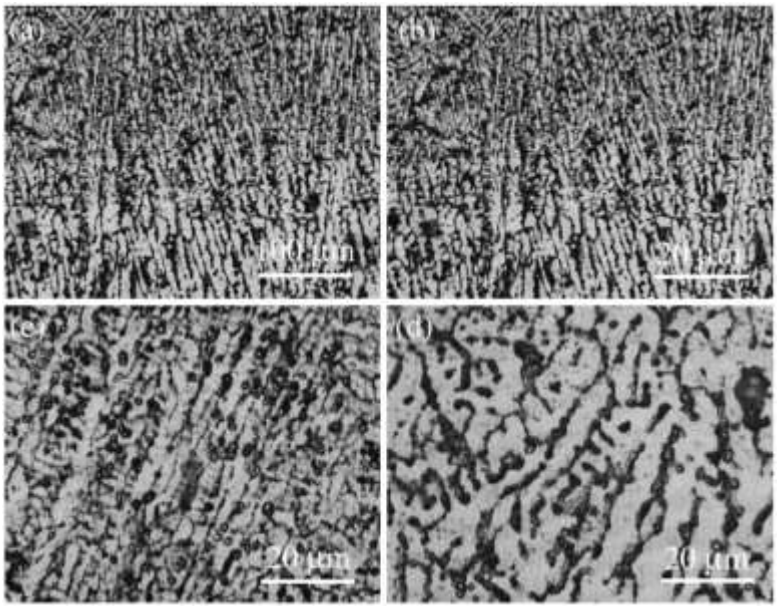

Figure 7: Microstructures of the deposited layers of 4043 Al-alloy: (a) an oriented growth in the middle or bottom part of the deposited layer; (b) precipitates at the grain boundaries; (c) equiaxed grains at the inside wall of the part; (d) equiaxed grains at the outside wall of the part [50]

Researchers at LKR explored variation in parameter sets for the cold metal transfer (CMT) process and their influence on the macro- and microstructure. Figure 8 shows the result of these three tests. Three specimens made from a ML5183 welding wire were produced. The chemical composition of the welding wire prior to the waDED processing in mass percent can be seen in Table 1. The overall surface appears to be smooth with a layer-like structure.

Table 1: Chemical composition of the ML5183 welding wire prior to waDED processing in mass percent[52]

Al	Mg	Mn	Cr	Cu	Fe	Si	Ti
93.9	5.03	0.64	0.08	0.02	0.16	0.05	0.09

The process parameters were varied and the respective changes in the outcomes were observed, these datasets can be seen in Table 2.

Table 2: Processing parameters used for the preparation of the three different material conditions[52]

Parameters	Parameters set no 1	Parameters set no 2	Parameters set no 2
Polarity variation	10:10	1:1	1:1
Mean wire feed rate v_{WF} (m/min)	5.2	5.2	4.5
Deposition rate, DR (kg/h)	0.94	0.94	0.81
Current $\bar{I}/I_{max}$ (A)	76 / 109	86 / 107	74 / 91
Mean voltage $\bar{U}$ (V)	8.6	12.4	10.6

Funded by the European Union. Views and opinions expressed are however those of the author(s) only and do not necessarily reflect those of the European Union or [name of the granting authority]. Neither the European Union nor the granting authority can be held responsible for them.

Travel speed (mms/s)	12	12	12
Energy input per unit length (J/mm)[a]	56	90	67

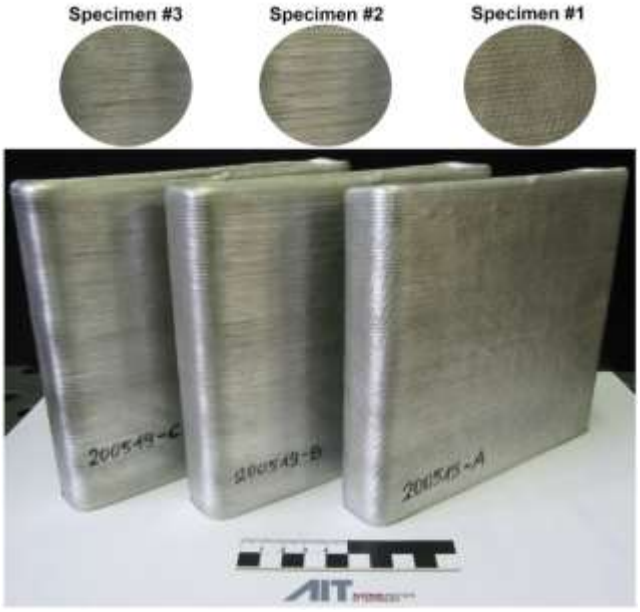

Figure 8: three waDED specimens manufactured with varying parameter sets[52]

The microstructure of specimen #1 is shown in Figure 9. This shows that a fine-grained region formed directly above the visible fusion penetration marks. This finer grain size originates from the high cooling rates in the bottom layer, followed by an elongated-grained structure, which grows perpendicular to the thermal gradient of the melt pool. The last area has a coarser grain, these grains are not elongated in a preferred direction, unlike those in the previous area.[52]

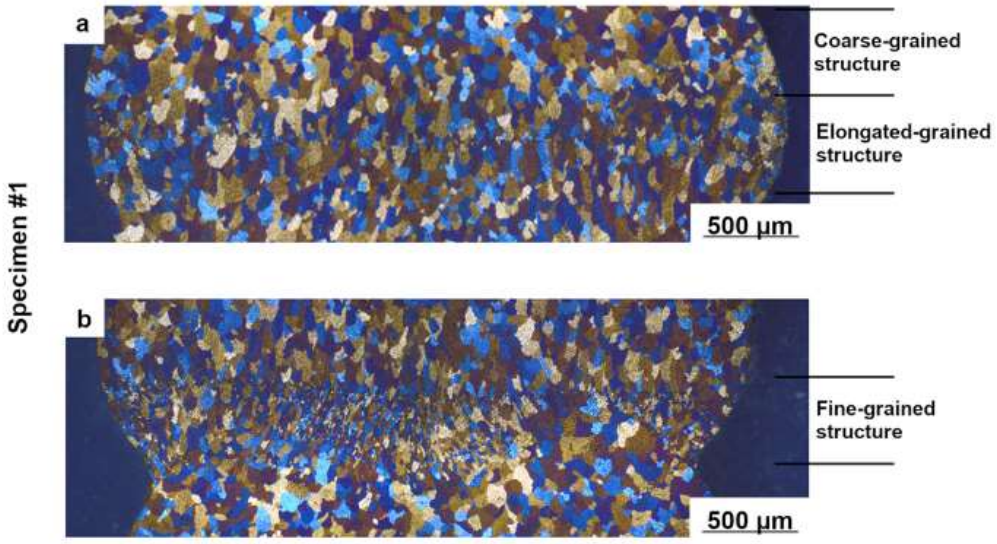

Figure 9: Microstructure waDED specimen #1 by LKR, a) Microstructure within the welded area, b) Microstructure inside the fusion zone between two consecutive areas [52]

Funded by the European Union. Views and opinions expressed are however those of the author(s) only and do not necessarily reflect those of the European Union or [name of the granting authority]. Neither the European Union nor the granting authority can be held responsible for them.

In contrast to that the specimen #2 (Figure 10) shows a more homogeneous grain structure, aside from small areas with a finer grain structure due to higher cooling rates which occur locally.

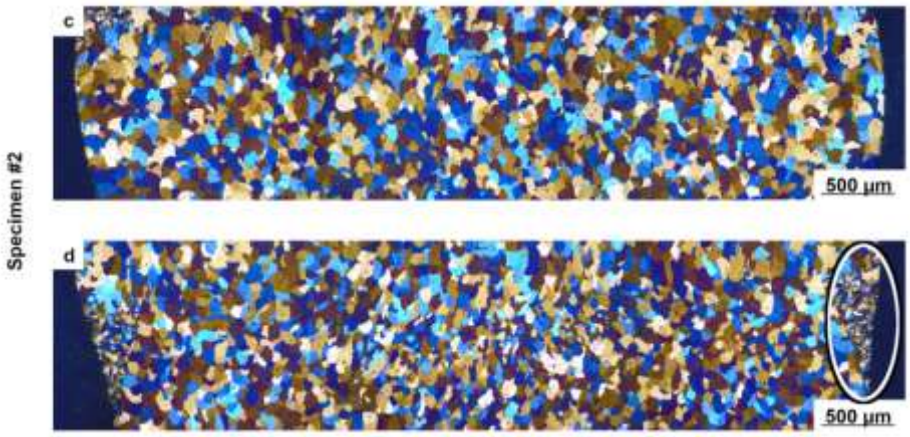

Figure 10: Microstructure waDED specimen #2 by LKR, a) Microstructure within the welded area, b) Microstructure inside the fusion zone between two consecutive areas [52]

Compared to sheet metal, the microstructure formation during waDED of aluminium are rather complex. Each deposited layer undergoes a unique thermal procedure, resulting in a different grain structure. In the CMT process this heat input can be controlled by the variation of the polarity and pulse repetition sequence. In general, a lower heat input can result in a finer and more homogeneous morphology of the microstructural features [52]

4.5.1.2 Magnesium

Magnesium alloys face the same problems during waDED processing as aluminium alloys, such as repetitive thermal exposure, steep thermal gradient resulting in elongated grains and anisotropic mechanical properties. Additionally, the low vapor pressure, low boiling point and high affinity for oxidation add additional challenges to waDED of magnesium alloys[53]. Furthermore, only a limited number of magnesium alloys are commercially available as filler metal. Reported alloys include AZ31B, AZ61A, AZ91D, EZ33A, AZ101A, QE22A, AM50A, and AZ92A[54], although their availability is oftentimes limited to the chinese or american market.

Nevertheless, a handful successful studies using Mg alloys have been performed attesting the suitability of waDED and demonstrating the lightweight construction potential.

Klein et al. demonstrate that the magnesium casting alloy AZ61 can be successfully processed via waDED. Using a CMT-based process, they were able to achieve a predominantly equiaxed grain morphology and superior mechanical properties compared to conventional casting processes[53].

Gneiger et al. used the magnesium alloys AEX11 and AZ61 for their waDED studies. They showed that the higher alloying content in the AEX11 can be capitalized on, due to the high cooling rates in waDED, and offer increased strength values compared to AZ61, especially in T6 condition[54].

4.5.2 Heat treatment

4.5.2.1 Solution heat treatment and artificial aging

Heat treatment is an important process in the production of aluminium alloys, and it involves a series of steps to improve their mechanical properties. Heat treatment is used to improve the strength, ductility, and toughness of these alloys, making them suitable for a wide range of applications.

Funded by the European Union. Views and opinions expressed are however those of the author(s) only and do not necessarily reflect those of the European Union or [name of the granting authority]. Neither the European Union nor the granting authority can be held responsible for them.

Aluminium alloys are classified as heat treatable and non-heat treatable depending on how well they respond to artificial aging i.e., precipitation hardening. Normally, the 2XXX, 6XXX and 7XXX are considered heat treatable, whereas the 1xxx, 3xxx, 4xxx and 5xxx fall into the group of non-heat treatable alloys.

The heat treatment process for aluminium alloys usually consists of two main steps: solution heat treatment and artificial aging.

Solution Heat Treatment: The first step of the heat treatment process is solution heat treatment, which involves heating the alloy to a specific temperature and holding it there for a certain period of time. The purpose of this step is to dissolve the alloying elements, which are typically present in a solid solution in the aluminium matrix. This is necessary because the strength of the alloy is dependent on the distribution and concentration of these elements, which are added to the aluminium to enhance its properties.

The temperature and duration of the solution heat treatment depend on the specific alloy being treated. For example, the common aluminium alloy 6061 requires a solution heat treatment at around 530 °C for about one hour, while the high-strength aluminium alloy 7075 requires a solution heat treatment at around 475 °C for several hours.

After the alloy has been heated to the desired temperature and held there for the required duration, it is then rapidly quenched in water or other quenching media to cool it down quickly. This prevents the alloying elements from precipitating out of the solution, which would reduce the strength of the alloy.

Artificial Aging: The second step of the heat treatment process is artificial aging, which involves heating the alloy to a lower temperature than that used in solution heat treatment. The purpose of this step is to allow the alloying elements to precipitate out of the solid solution and form small, evenly distributed particles throughout the aluminium matrix. This results in an increase in the strength and hardness of the alloy.

The temperature and duration of the artificial aging process also depend on the specific alloy being treated. For example, the common aluminium alloy 6061 requires an artificial aging process at around 160 °C for several hours, while the high-strength aluminium alloy 7075 requires an artificial aging process at around 120 °C for several hours.

During the artificial aging process, the alloy is heated to the desired temperature and held there for the required duration. This allows the alloying elements to form small, evenly distributed particles throughout the aluminium matrix, which results in an increase in the strength and hardness of the alloy.

4.5.2.2 Stress relief heat treatment

Stress relief heat treatment is used when a component is subjected to uneven temperature effects, causing stresses. Processes that cause uneven heating, deformation or cooling, such as casting and welding, cause these stresses. Aluminium is usually exposed to temperatures of 200°C to 300°C during stress relief heat treatment. Non-age-hardenable alloys can be stress-relieved at a soft annealing temperature of 350°C. In the case of heat-treatable alloys, stress-relief heat treatment can cause a change in the microstructure and thus in the strength[55].

4.5.3 Manufacturing processes and consumables

4.5.3.1 Manufacturing processes

Depending on the heat source, the waDED processes can be separated into three groups: Gas Metal Arc Welding (GMAW)-based, Gas Tungsten Arc Welding (GTAW)-based, and Plasma Arc Welding (PAW)-based.

Funded by the European Union. Views and opinions expressed are however those of the author(s) only and do not necessarily reflect those of the European Union or [name of the granting authority]. Neither the European Union nor the granting authority can be held responsible for them.

Each system has its advantages and disadvantages when compared to the others. The table shown in Figure 11 gives an overlook on the processes and their features.

WAAM	Energy source	Features
GTAW-based	GTAW	Non-consumable electrode; Separate wire feed process; Typical deposition rate: 1-2 kg/hour; Wire and torch rotation are needed;
GMAW-based	GMAW	Consumable wire electrode; Typical deposition rate 3-4 kg/hour; Poor arc stability, spatter;
	Cold metal transfer (CMT)	Reciprocating consumable wire electrode; Typical deposition rate: 2-3 kg/hour; Low heat input process with zero spatter, high process tolerance;
	Tandem GMAW	Two consumable wires electrodes; Typical deposition: 6-8 kg/hour; Easy mixing to control composition for intermetallic materials manufacturing ;
PAW-based	Plasma	Non-consumable electrode; Separate wire feed process; Typical deposition rate 2-4 kg/hour; Wire and torch rotation are needed;

Figure 11: Comparison of the various waDED techniques[56]

The overall quality of a product produced with the waDED process relies on multiple aspects. The most important ones are the selection of the right process, the quality of the wire and the post process treatment, these and some more are displayed in Figure 12.

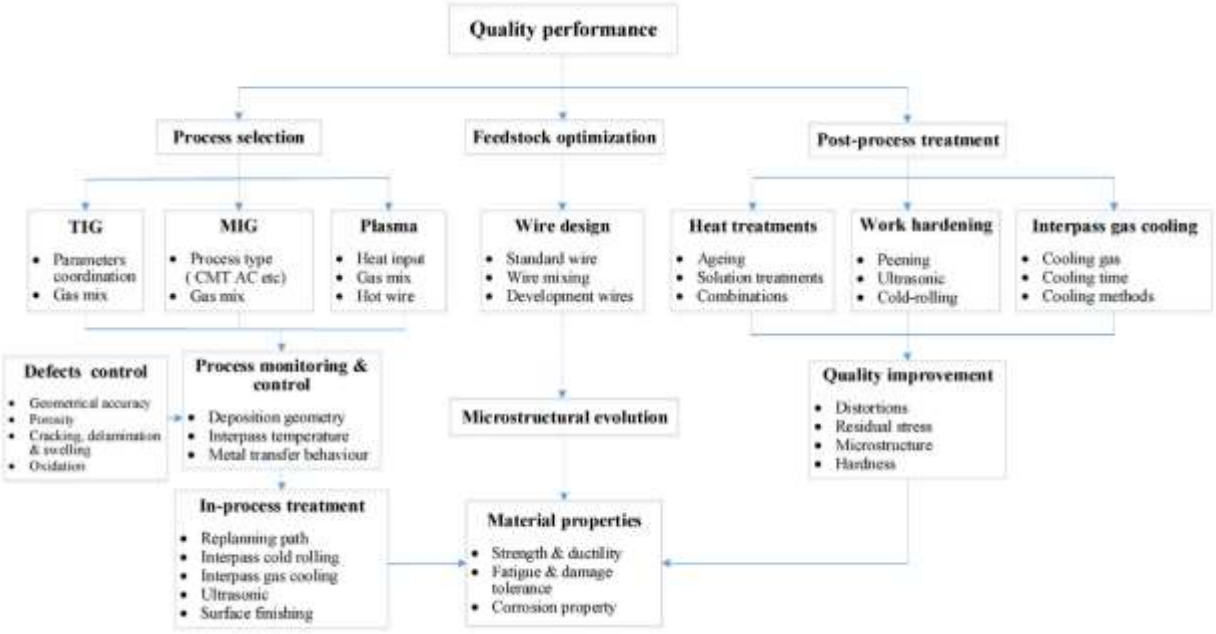

Figure 12: A quality-based framework for the waDED process[56]

Funded by the European Union. Views and opinions expressed are however those of the author(s) only and do not necessarily reflect those of the European Union or [name of the granting authority]. Neither the European Union nor the granting authority can be held responsible for them.

The choice of the production technique depends on the processing conditions, the feedstock and production rate for the target component. Furthermore, the motion mechanism in most waDED systems is a multi-axle industrial robot, carrying the torch.

The production of a waDED part includes three main steps. The process planning, which involves the creation of the CAD model, the 3D slicing of the 3D model into layers, the creation of the program including the robot motions and the welding parameters, the deposition of the welding material itself with process controlling and the post processing including the evaluation of the result, possible finish and if necessary, path re-planning.

4.5.3.2 Consumables

The feedstock is one of the biggest advantages the wire-based processes have over the powder-based processes. The handling of the wire is easier and less of a health risk than that of powder. The consumables for waDED processes include commercially available wires produced for the welding industry and are available in spooled form. The most commonly used metals include Ti-, Al-, Steel- and Ni-based alloys[56]. Furthermore, non-commercially available wires can be produced in small batches on demand.

Porosity affects additively manufactured aluminium. This porosity can be minimized employing a mix of high-quality welding wires and specific synergistic operating modes. In particular Fronius cold metal transfer (CMT) process and its pulsed advanced variant yields good results due to lower heat input, which results in lower finer equiaxed grains and effective oxide cleaning of wire and substrate[57,58].

In terms of welding wires made from aluminium and aluminium alloys a small variety of products is available on the European market, mostly 4XXX, 5XXX and some 1XXX and 2XXX (1070, 1450, 2319, 4018, 4020, 4043, 4046, 4047, 5087, 5183, 5356, 6063).

For magnesium alloys the choice of filler metals is even smaller as mentioned above. Available alloys include AZ31B, AZ61A, AZ91D, EZ33A, AZ101A, QE22A, AM50A, and AZ92A, although their availability is oftentimes limited to the chinese or american market.

4.5.4 Implications of microstructure on hydrogen performance

Although solid solubility of hydrogen in bulk aluminum under atmospheric hydrogen pressure is extremely low, aluminum and its alloys usually contain about ten times as much hydrogen amount as the solubility limit[59]. However, a main factor in the microstructure of the aluminum alloys which controls the effect of the hydrogen, in fact, is that lattice transport of hydrogen is extremely slow in aluminum, making it difficult to the hydrogen to be able to keep up with a moving crack, or be transported to a crack region by volume diffusion.

The various aspects of hydrogen in materials have been previously studied extensively[60]. It was shown that the microstructural driven hydrogen trapping can also influence the hydrogen embrittlement resistance of the aluminum alloys. This is because of the fact that the microstructural defects such as interstitial lattices, vacancies, dislocations and solute atoms strongly influence the movement of hydrogen atoms and the content of trapped hydrogen inside the aluminum alloys[61]. In general, trapping sites for hydrogen are classified as reversible or diffusible trapping sites, and irreversible or non-diffusible trap sites. Thus, the microstructural defects can also change the effective distribution, retention and diffusivity of the hydrogen in microstructures.

4.5.5 Implications of microstructure on cryogenic performance

There has been a significant amount of research done about the suitability of aluminium alloys for pressure vessel construction. An overview of the cryogenic characteristics of regularly utilized materials was provided by Hurlich[62], the mechanical properties of Face Centred Cubic (FCC) metals such as Al, Cu, and Ni, in sheet

Funded by the European Union. Views and opinions expressed are however those of the author(s) only and do not necessarily reflect those of the European Union or [name of the granting authority]. Neither the European Union nor the granting authority can be held responsible for them.

metal form, have been observed to improve when the temperature decreases to cryogenic levels. Slip systems in FCC metals allow dislocations to freely move along the close-packed planes. However, there are no close-packed planes in BCC metals that allow for simple dislocation migration, hence dislocation mobility in these materials (BCC metals) requires heat activation to slide. Otherwise, the material adapts to the imposed stress by more extreme processes, such as bond breakage[63].

From the literature it can be concluded that the microstructure and mechanical behaviour of aluminium alloys is influenced by cryogenic treatments. Cryogenic treatments can increase the homogeneity in the microstructure of the material, which leads to improved strength and hardness. Depending on the duration of the cryo treatment the grain size of the material decreases[64,65].

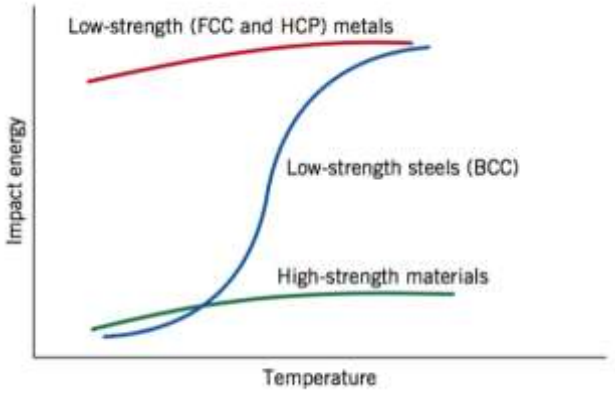

Figure 13: Ductile to brittle transition temperature comparison of metals with different microstructure[66]

The literature specifically mentions the usage of 2024-T4, 2219-T87, 5052 H38, 5083 H38, and 6061-T6 aluminium alloys for the fabrication of pressure vessels for the storage of liquid hydrogen. In that article, the cryogenic mechanical characteristics of the aluminium alloys stated were not compared in depth. The researchers at LKR did a literature study on the influence of cryogenic temperatures on the mechanical properties of the 2024-T4, 2024-T6, 2219-T87, 5052 H38, 5083-H38, 6061-T6, 6063 T6, 7039-T63 and T7075-T73 aluminium alloys. Data which was fitting the given circumstances with a focus on the tensile strength, the yield strength and the elongation were compared.

4.5.5.1 Tensile strength

The characterisation of the tensile strength of the above-mentioned aluminium alloys under the given conditions, were tested applying the ASTM B 557- E8[67] standard. The samples were submerged for a period of time in cryostats containing various fluids such as dry ice and alcohol for -28 °C, liquid petroleum for -80 °C, liquefied nitrogen for -196 °C, and liquefied hydrogen for -253 °[68]. The reference points created this way are displayed in Figure 14, there the tensile strength as a function of the temperature is shown for a temperature range from -253 °C up to 400 °C. The overall trend indicates an increase in tensile strength at decreasing temperature. This behaviour can be observed in all the alloys tested.

Funded by the European Union. Views and opinions expressed are however those of the author(s) only and do not necessarily reflect those of the European Union or [name of the granting authority]. Neither the European Union nor the granting authority can be held responsible for them.

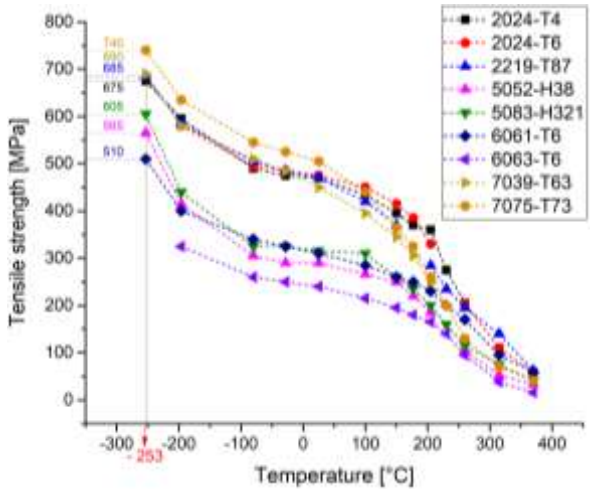

Figure 14: A comparison between temperature dependent tensile strength of aluminium alloys 2024-T4, 2024-T6, 2219-T87, 5052-H38, 5083-H321, 6061-T6, 6063-T6, 7039-T63 and 7075-T73 at -253 °C

4.5.5.2 Yield strength

Using the same cryostats as reference points, Figure 15 outlines the yield strength based on various temperatures for the aluminium alloys 2024-T4, 2024-T6, 2219-T87, 5083-H321, 5052-H38, 6061-T6, 6063-T6, 7039-T63 and 7075-T73. Following the pattern of the tensile strength, the yield strength also increases with decreasing temperature. The 2xxx- and 7xxx series alloys exhibit the strongest temperature dependency.

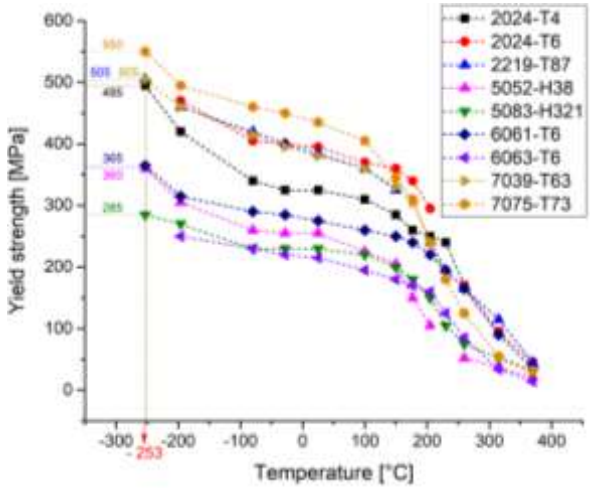

Figure 15: A comparison between temperature dependent yield strength of aluminium alloys 2024-T4, 2024-T6, 2219-T87, 5052-H38, 5083-H321, 6061-T6, 6063-T6, 7039-T63 and 7075-T73 at -253 °C

4.5.5.3 Elongation in 4D

Elongation in 4D refers to the elongation test where the gauge length for circular specimens is four times longer than their diameter, according to the ASTME8/E8M 13a standard[69]. This is an indicator of the ductility of a material. Figure 16 depicts the temperature dependence of the elongation in 4D for the aluminium alloys 2024-T4, 2024-T6, 2219-T87, 5083-H321, 5052-H38, 6061-T6, 6063-T6, 7039-T63, and 7075-T73.

Funded by the European Union. Views and opinions expressed are however those of the author(s) only and do not necessarily reflect those of the European Union or [name of the granting authority]. Neither the European Union nor the granting authority can be held responsible for them.

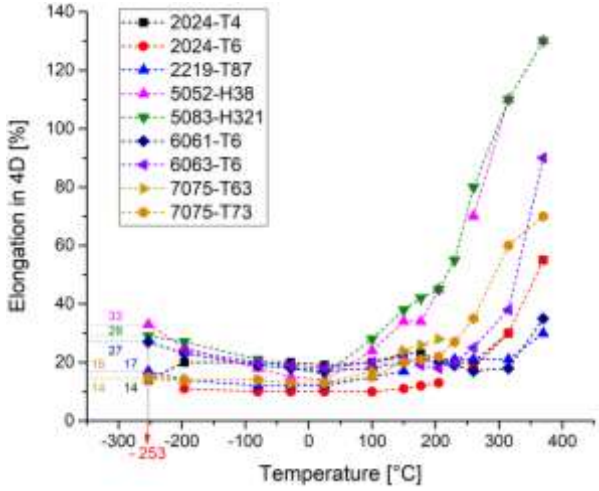

Figure 16: A comparison between temperature dependent elongation in 4D of aluminium alloys 2024-T4, 2024-T6, 2219-T87, 5052-H38, 5083-H321, 6061-T6, 6063-T6, 7039-T63 and 7075-T73 at -253 °C

Funded by the European Union. Views and opinions expressed are however those of the author(s) only and do not necessarily reflect those of the European Union or [name of the granting authority]. Neither the European Union nor the granting authority can be held responsible for them.

4.6 COATINGS LITERATURE REVIEW

In this project, coatings applied over waDED alloys, are intent to work as a barrier, to enhance its hydrogen embrittlement resistance and stress cracking corrosion (SCC) resistance. From a literature review a lack of literature was available on this matter; however, some type of coatings, applicability and hydrogen evaluations were found and described below as the best way to overcome the project´s challenges.

4.6.1 Type of coating and applicability

4.6.1.1 Epoxy

Epoxy resins are characterized by a three-membered ring known as the epoxy, epoxide, oxirane, or ethoxyline group:

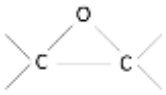

Commercial epoxy resins contain aliphatic, cycloaliphatic, or aromatic backbones. The capability of the epoxy ring to react with a variety of substances imparts versatility to the resins. Treatment with curing agents gives insoluble and intractable thermoset polymers. To facilitate processing and modify cured resin properties, other constituents may be included in the compositions: fillers, solvents, diluents, plasticizers, and accelerators.

High chemical and corrosion resistance, good mechanical and thermal properties, outstanding adhesion to various substrates, low shrinkage upon cure, flexibility, good electrical properties, and ability to be processed under a variety of conditions are characteristics of epoxy resins[70].

A literature review was done by using the CAS SciFinder^n website. In the Table 3 is shown the literature review of epoxy coatings used in hydrogen storage.

Table 3. Literature review – Epoxy Coatings

CAS SciFinder^n

Keywords	Search within results		Results	Relevants
Epoxy properties	+	Cryogenic conditions, hydrogen embrittlement & epoxy coating	7	2
Epoxy Coating	+	Aluminium alloy & corrosion protection	85	0
Epoxy Coating	+	Aluminium alloy, corrosion protection & “hydrogen storage”	0	0

From this literature review, 2 relevant papers were identified, as described below.

Hydrogen embrittlement is a very important phenomenon which causes the high strength steel to fail below its permissible limit. These high strength materials are used in various industries such as power, nuclear, transport, aerospace, marine, hydrogen storage tanks etc. Hydrogen may diffuse in high strength material either internally during the manufacturing stage or externally from environment during application. Due to this hydrogen diffusion the service life of many high strength components like pressure vessels, fasteners & other stressed members may be reduced and result in unexpected failure. An attempt has been made by *Khare A. et*

Funded by the European Union. Views and opinions expressed are however those of the author(s) only and do not necessarily reflect those of the European Union or [name of the granting authority]. Neither the European Union nor the granting authority can be held responsible for them.

al[71] to use the conventional tensile and impact test methods to determine the effect of process behaviour on the properties of high strength steel. Specimens with different mechanical properties and heat treatment conditions were made to conduct the testing. This study determines the impact of coating especially the zinc coating process on mechanical properties of the material. Further hydrogen embrittlement prevention and development of new coatings were discussed.

Niermann, Dirk et al.[72] studied the typical properties of epoxy resin compared regarding temperature application range, initial shear strength and strain limit. The aging behaviour of an adhesive joint can be improved by surface pre-treatment of the titanium parts in an alk. pickling, bath containing tartrates which removes the oxide layer and avoids hydrogen embrittlement.

It is interesting that searching literature for *epoxy coatings + aluminium alloy and corrosion protection* is possible to find 85 publications, however, if *"hydrogen storage"* keyword is added, there are no results obtained. This fact is due to a lack of literature relating coatings + aluminium alloys + corrosion & hydrogen storage applications.

Furthermore, a web searching was done looking for commercial products that have as operating condition the cryogenic temperature (-196 ºC). A key factor that must be fulfilled in parallel with other such as adhesion, corrosion resistance, among others. For this reason, Table 4 shows an overview of available commercial products in the market that can meet these requirements.

Table 4. Some of commercial products available (spray/brush application method)

Type of coatings for other final application	Working temperatures	Dry-film thickness	Application method	Commercial ID
A two-component polyamine cured phenolic/novolac epoxy coating	From 205 ºC to -196 ºC	100 – 200 µm	Airless spray and brush	Epoxy HR (JOTUN)[73]
A two-component glass flake reinforced epoxy composite coating	From 250 ºC to -196 ºC	140 – 200 µm	Airless spray and brush	Jotatemp 250 (JOTUN)[74]
A three-component titanium catalyzed inorganic ceramic copolymer-based coating	From 1000 ºC to -196 ºC	100 – 150 µm	Airless spray and brush	Jotatemp 1000 (JOTUN)[75]
Modified epoxy phenolic, amine adduct cured	From 204 ºC to -196 ºC	127 – 152 µm per coat (primer and finish)	Airless spray and brush	Thermaline® 440 (Carboline)[76]
A high-performance alkylamine-cured epoxy	From 275 ºC to -196 ºC	150 µm	Airless spray and brush	Hempaprime CUI 275 (HEMPEL)[77]

These protective coatings, epoxy coatings, are designed as corrosion protection for surfaces operating at extreme temperatures where long corrosion protection is desired. The products can be applied by airless spray or brush for small areas. To secure lasting adhesion a surface preparation must be done. Surface shall be clean, dry, and free from any contamination. A recommended surface preparation involves an abrasive blast cleaning to achieve a surface profile using non-metallic abrasive media which is suitable to achieve a sharp/angular surface profile.

Funded by the European Union. Views and opinions expressed are however those of the author(s) only and do not necessarily reflect those of the European Union or [name of the granting authority]. Neither the European Union nor the granting authority can be held responsible for them.

On the other hand, instead of spray or brush application, electrocoats can be a great product to fulfil the requirements, see Table 5.

Table 5. Commercial product available (e-coating/anaphoretic deposition as application method)

Type of coating for other application	Cryo-Temp	Dry-film thickness	Application method	Commercial ID
Anionic epoxy electrocoat	-50 ºC, however, -196 ºC must be tested.	20 µm	e-coating/anaphoretic deposition	Aerocron™ 2100 from PPG[78]

Aerocron™ 2100 is an anionic epoxy electrocoat primer technology designed to provide optimal corrosion protection over aluminium substrates (aircraft applications). It is a chrome-free, water-based technology that is applied via an immersion process which uses electrical current to deposit the coating onto a conductive substrate. Electrocoat process also provides advantages over spray technology with increased productivity, increased transfer efficiency rate of parts, full automation capabilities, lower waste disposal costs, and uniform thickness which results in an overall weight reduction[78]. However, Aerocron™ 2100 (PPG) is not tested at cryogenic temperatures which is a critical requirement in the project. For this reason, testing at cryogenic temperatures will be included in the first stage of the project.

4.6.1.2 PTFE

Polytetrafluoroethylene (PTFE) has a unique position in the plastics industry due to its chemical inertness, heat resistance, excellent electrical insulation properties, and the low coefficient of friction in a wide temperatures range. Polymerization of tetrafluoroethylene (TFE) monomer gives this perfluorinated straight-chain high polymer with the formula $-(CF_2 - CF_2)_n -$. Its high thermal stability is due to the strong carbon-fluorine bond and characterizes PTFE as a very useful high temperature polymer. Because of its chemical inertness and high molecular weight, PTFE does not flow and cannot be fabricated by conventional techniques[70].

A literature review was done by using the CAS SciFinder^n website. In the Table 6 is shown the literature review of PTFE coatings used in hydrogen storage.

Table 6. Literature Review – PTFE Coatings

CAS SciFinder^n

Keywords	Search within results		Results	Relevants
Coating	+	"Hydrogen storage", Lightweight alloys, Polytetrafluoroethylene (PTFE) or Teflon & Exclude: "Hydrogen storage alloy"	17	1
PTFE Coating	+	"Hydrogen storage" & "PTFE Coating"	3	2

From this literature review, 3 relevant papers were identified, as described below.

A review of metallic tanks for H_2 storage has been made by *Wang Z et al*[79], where hydrogen is showed as a promising option for alternative fuels and/or energy sources for future ships. This review focuses on the mechanical testing, selection of materials and failure mechanisms for cryo-compressed and liquid hydrogen tanks and their insulations. Knowledges gaps are identified to facilitate further research and development in this field. Additionally, coatings are mentioned in page 21, where is indicated that polytetrafluoroethylene (PTFE)

Funded by the European Union. Views and opinions expressed are however those of the author(s) only and do not necessarily reflect those of the European Union or [name of the granting authority]. Neither the European Union nor the granting authority can be held responsible for them.

coating further enhances the hydrogen embrittlement resistance of austenitic stainless steels for LH_2 tanks[80].

Hwang J-S et al[80] studied the polytetrafluoroethylene (PTFE), which is known to be an effective hydrogen adsorption and desorption material, was coated on the surface of stainless steel 304 to improve its hydrogen embrittlement resistance. To investigate the effects of PTFE coating on the hydrogen embrittlement resistance on stainless steel 304, the Charpy V-notch impact (CVN) test was performed under three different temperatures: 25, -83, and -196 ºC. Additionally, hydrogen concentration, electron back scatter diffraction (EBSD), and scanning electron microscopy (SEM) evaluations were carried out to verify the results of the CVN impact test. The PTFE coating did not have a significant effect on the quantitative reduction of hydrogen concentration; however, they confirmed its excellent performance in terms of toughness reduction due to the increase in hydrogen loading time at room temperature.

Ngene P. et al[81] stated the catalytic properties of Pd alloy thin films are enhanced by a thin sputtered PTFE coating, resulting in profound improvements in hydrogen adsorption and desorption in Pd-based and Pd-catalyzed hydrogen sensors and hydrogen storage materials. The remarkably enhanced catalytic performance is attributed to chemical modifications of the catalyst surface by the sputtered PTFE leading to a possible change in the binding strength of the intermediate species involved in the hydrogen sorption process.

4.6.1.3 Polyurethane

The polymers known as polyurethanes include materials that incorporate the carbamate functional group as well as other functional groups, such as ester, ether, amide, and urea. They are usually produced by the reaction of polyfunctional isocyanates, most often with hydroxyl compounds. Since the functionality of hydroxyl-containing reactant or the isocyanate can be variated, a wide variety of branched or cross-linked polymers can be formed. The polyfunctional isocyanates can be aromatic, aliphatic, cycloaliphatic, or polycyclic in structure and can be used directly as produced or modified. This flexibility in the selection of reactants leads to the wide range of physical properties that allows polyurethanes to play an important role in the world market for quality products from synthetic polymer[70].

Polyurethane coatings are preferred for many applications because of a unique combination of performance and application properties. These products provide excellent abrasion resistance, flexibility, hardness, and chemical and solvent resistance; light stability and weatherability are excellent. Most polyurethane coatings are referred to as reactive coatings because lower molecular weight oligomers react to form a polymeric network on the substrate; energy requirements for cure are low[70].

A literature review was done by using the CAS SciFinder^n website. In the Table 7 is shown the literature review of Polyurethane coatings used in hydrogen storage.

Table 7. Literature review – Polyurethane Coatings

CAS SciFinder^n

Keywords	Search within results		Results	Relevants
Polyurethane	+	"Cryogenic", coating & corrosion	2	2
Polyurethane Coating	+	"Hydrogen storage", "hydrogen embrittlement" & "polyurethane"	4	0

Funded by the European Union. Views and opinions expressed are however those of the author(s) only and do not necessarily reflect those of the European Union or [name of the granting authority]. Neither the European Union nor the granting authority can be held responsible for them.

Polyurethane Coating	+	"Hydrogen storage", "hydrogen embrittlement" & lightweight alloys	1	0

From this literature review, 2 relevant papers were identified, as described below.

According to *Narain, S.*[82] coatings have been accepted as a highly effective method for protecting insulated austenitic stainless-steel equipment and piping against chloride stress corrosion cracking. In liquefied natural gas (LNG) plants, coating systems should be suitable for low-temperature conditions down to -160 °C. A comprehensive cryogenic test program was undertaken to gather information on the low-temperature performance of shop-applied coatings. This included cycling from atm. temperatures to cryogenic temperatures and reverse cycling. Cryogenically cycled test samples were evaluated by visual examination, adhesion, and impact tests. The test results gave increased confidence in shop-applied coating systems. The test as performed provided a reasonable screening method for coating systems used in the cryogenic cycling conditions of LNG plants.

Kumar K. et al[83] presented an epoxy-polyurethane coating for corrosion prevention of machinery in an acrylic fiber plant by HNO_3. Chlorinated rubber coatings were best for cryogenic containers and stainless steel-carbon steel joints of heat exchangers. High-build polyurethane coatings gave good protection to metals and others in cooling towers and screw conveyors.

4.6.2 Hydrogen diffusion and permeation

A literature review was done by using the CAS SciFinder^n website. In the Table 8 is shown the literature review of coatings and aluminium alloys used in hydrogen storage.

Table 8. Literature review – Coatings & Aluminium Alloys

CAS SciFinder^n

Keywords	Search within results		Results	Relevants
Coatings	+	"Aluminium alloys", "hydrogen storage" & hydrogen embrittlement	2	1

A review of analysis of hydrogen embrittlement on aluminium alloys for vehicle-mounted hydrogen storage reported by *Chen Y. et al*[84] is showing methods of prevention such as coatings. Included in this paper, *Dey S. et al*[85] proposed some improvement schemes to limit the diffusion depth of H in the material. Many scholars have proposed that coating is also based on the depth of H diffusion in the material. Therefore, when proposing structural measures for HE, it is necessary to study the mechanism and main influencing factors of HE carefully.

In terms of prevention of hydrogen embrittlement *Chen Y. et al*[84] also indicated that to guarantee safety, selection of the suitable prevention techniques becomes important. The prevention methods proposed by scholars in the past can be divided into two ideas. One is to block hydrogen from the material, that means using inhibition of film formation on aluminium alloy surface or coating methods. The other is to treat the material to make it more resistant to HE, including heat treatment methods and refining grain methods.

Funded by the European Union. Views and opinions expressed are however those of the author(s) only and do not necessarily reflect those of the European Union or [name of the granting authority]. Neither the European Union nor the granting authority can be held responsible for them.

4.7 HYDROGEN TESTING METHODOLOGIES

4.7.1 Introduction

The MAST3RBoost project aims developing a hydrogen storage system based on adsorption process at comparatively low compression (100bar or below), which could be an alternative to state-of-the-art compressed gaseous hydrogen systems at 350bar or more used in the transport sector. The vessel for the storage system will be fabricated using wire+arc additive manufacturing and it will be made from lightweight Al and Mg based alloys, i.e. so called Type I pressure vessel[86].

Although MAST3RBoost project is limited to building a demonstration model, any commercial product in the future is expected to comply with pressure vessel industry rules and regulations. Thus, the section starts reviewing the requirements for an industry compliant pressure vessel design, then it continues with individual mechanical testing standards to obtain the required material properties.

This literature review does not aim to provide an exhaustive list of material and component testing options in hydrogen environment, but rather it presents a targeted information with respect to MAST3RBoost structural design specification, e.g. pressure vessel fabricated from lightweight metallic alloys subject to a maximum 100bar hydrogen pressure at minimum -196.15°C (77K) temperature. Thus, recommendations for general hydrogen service, e.g. (ANSI/CSA, 2014 (R2018))[87], or design rules from other industries such as piping (ASME, 2020) are considered as outside of the scope.

4.7.2 Review of pressure vessel design practices for hydrogen service

At the time of the writing, a comprehensive industrial design practice is not available for pressure vessels intended for gaseous hydrogen storage (>10bar) at low temperatures.

H-3 publication[88] (CGA, 2019) from Compressed Gas Association (CGA) in North America is intended for cryogenic vessels for hydrogen service, albeit it is limited to liquid hydrogen at approximately 12bar pressure. Thus, this standard is not directly applicable in the MAST3RBoost project, where the design pressure is much higher, e.g. 100bar, and the physical state of the stored hydrogen is not liquid.

Similarly, European standards for cryogenic vessels do not cover MAST3RBoost operational requirements. Hydrogen fuel tank design practice[89] is intended for liquid hydrogen storage, i.e. low pressure applications. Static cryogenic vessel design practices[9091] are not intended for cyclic loads that could result fatigue type failure, whereas MAST3RBoost pressure vessel needs to be fatigue rated due to expected refuelling cycles. Transportable cryogenic vessel standard[92] considers fatigue loads but exclude hydrogen service. There is a separate standard (BSI, 2001) for material selection of cryogenic vessels; these standard states that hydrogen embrittlement normally occur at ambient temperatures and become negligible at cryogenic temperatures, then suggests that the design can be based on BS EN ISO 11114[93], which is a standard for pressure vessel design in hydrogen service except the cryogenic temperatures and is reviewed later on in this document.

At sufficiently low temperatures, the fracture mechanism can transition from ductile to brittle, hence the influence of cryogenic temperatures on fracture toughness needs to be determined via mechanical testing. The toughness requirements for materials to be used in cryogenic vessels are given in BS EN 1252-1[94]. This standard considers aluminium alloys as “inherently though” and thus find impact tests at low temperatures unnecessary to obtain an indication about fracture toughness. This statement is further corroborated in another standard[95] referred in pressure vessel codes, which states that all aluminium alloys given in Table 5.6-1 of the standard are suitable for any minimum temperature without impact testing.

Funded by the European Union. Views and opinions expressed are however those of the author(s) only and do not necessarily reflect those of the European Union or [name of the granting authority]. Neither the European Union nor the granting authority can be held responsible for them.

In general, it was observed that the cryogenic vessel codes either do not cover the operational requirements of the MAST3RBoost project or provide limited information about the possible hydrogen influence on mechanical properties. The remaining of this subsection continue with the design practices for pressure vessels in hydrogen service, but not necessarily for cryogenic temperatures.

ASME Boiler and Pressure Vessel Code (BPVC) Section VIII-3: Alternative Rules[96]

Pressure vessel design is based on brittle fracture or plastic collapse, hydrogen assisted cracking, and fatigue. For calculations based on yield and tensile strength, the standard provides minimum values for each alloy in Part KM. However, both hydrogen and cryogenic temperatures can influence the yield and tensile strength values. Therefore, before using the values provided in Part KM for any engineering assessment, it seems sensible to determine the influence of environmental conditions on yield and tensile strength by means of mechanical testing.

Article KD-10 within this standard provides fatigue and fracture toughness requirements for pressure vessels in hydrogen service, which are additional to the requirements given in the main body of the standard. The article distinguishes welded and non-welded vessels; it can be assumed that wire+arc additive manufacturing, which is the processing technique of the MAST3RBoost project, is more analogous to a welded vessel type[97,98]. The additional requirements given in KD-10 are mandatory for welded vessels operating below 95 °C and above 170bar operating pressure, which reduces to 52bar if the tensile strength of vessel material exceeds 620MPa.

The material choice of the standard for a lightweight alloy is Al6061 series with either T6 or T651 temper as tabulated in Table KM-400 along with minimum yield and tensile strength values. Article KD-10 explicitly states that for aluminium alloys the effect of hydrogen on fatigue and fracture properties can be neglected. This statement is further corroborated by ISO 15916[99], which classifies aluminium alloys and specifically Al6061-T6 alloy as “negligibly embrittled” in Tables C1-2 of the standard. Here, it is important to underscore that hydrogen embrittlement depends on environmental conditions and given that these standards do not cover cryogenic temperatures, the statement of aluminium alloys cannot necessarily be extrapolated to MAST3RBoost operating conditions without further mechanical testing.

Although both total life (S-N approach) and fracture mechanics approaches are allowed in the main body of the ASME BPVC[96] Section VIII-3, for pressure vessels intended for hydrogen service, fatigue assessment must be carried out using a fracture mechanics approach as specified in Article KD-10. The allowable number of cycles, i.e. fatigue endurance, is calculated by propagating an initial flaw size to a critical flaw size. Article KD-10 specifies a single stage crack growth law that where the Paris law constants, C and m, must be determined in a hydrogen environment. The critical flaw size is determined by using the Failure Assessment Diagram (FAD), which is constructed by plane-strain fracture toughness, KIc, or by threshold stress intensity factor for hydrogen assisted cracking, KIH, whichever is smaller.

Threshold stress intensity factor for hydrogen assisted cracking, KIH, is to be determined by broadly following the ASTM E1681[100] standard using either constant load or constant displacement approach in hydrogen environment at vessel design pressure. More information regarding these test approaches can be found later in the document when discussing about material testing standards. Test duration is specified as 1,000 hours for ferritic steels and martensitic stainless steels, and 5,000 hours for austenitic steels at room temperature. There are no specific instructions available for aluminium alloys, which is most likely related to the statement that the Article KD-10 does not consider aluminium alloys susceptible to hydrogen embrittlement. Three test replications are recommended to establish KIH value, and the test specimen thickness must be comparable in size to the thickest part of the pressure vessel.

Funded by the European Union. Views and opinions expressed are however those of the author(s) only and do not necessarily reflect those of the European Union or [name of the granting authority]. Neither the European Union nor the granting authority can be held responsible for them.

Fatigue crack growth rate testing to follow ASTM E647 standard[101] in hydrogen environment at vessel design pressure. Test specimen is to be extracted from LT direction according to ASTM E399[102] with a mechanically introduced surface notch. A maximum test frequency of 0.1Hz was specified, and the R-ratio, which is defined as Kmin /Kmax, to be equal or larger than service conditions. Here, it is important to underscore that the specified test frequency is extremely low, which can lead to many months of testing. Depending on the application, both increasing and decreasing ΔK tests will be most likely to be required to generate a sufficient da/dN versus ΔK curve that covers mechanical design loads. Similar to fracture toughness testing, three test replications were recommended for fatigue crack growth testing.

For both fatigue crack growth rate and fracture toughness testing, the Article KD-10 specifies a high purity environment without air and moisture with a gas composition of 99.9999% hydrogen.

BS EN ISO 11114 - Gas cylinders[93]

This international standard provides recommendations for pressure vessels, or gas cylinders as referred in the standard, which will be subject to a non-inert gaseous service, including hydrogen gas. Part 1 of the standard provides guidance on material selection, and Part 4 outlines mechanical testing methods for selecting steels resistant to hydrogen embrittlement within defined operating and environmental conditions.

Aluminium alloys are classified as “acceptable” by Part 1 for the hydrogen service; the standard then refers to another document, BS EN ISO 7866[103], for specific aluminium alloy grades. Apart from Al6061 alloy as specified in KD-10 of ASME BPVC[96] Section VIII-3, the provided material list is more comprehensive and includes aluminium alloys from 2xxx series, 5xxx series, and 7xxx series.

Part 4 of the standard provides three different test methods to qualify steels that fall outside the basic criteria given in Part 1, e.g. steels with tensile strength higher than 950MPa. As stated in the beginning of Part 4, the provided test methods are only intended for seamless steel material, i.e. not applicable to light alloys or wire+arc additive manufacturing that are the material and processing choice in MAST3RBoost project. Although three different test methods are provided, they are all pass/fail decision types of mechanical tests. In contrast, mechanical testing requirements in KD-10[96] are intended to support subsequent engineering calculations.

The first test method, “Disc Test”, consists of subjecting a 58mm diameter thin disc in two different compressed gas environments: hydrogen and helium, which the latter is considered as inert. Gas pressure is increased at a constant rate during the test until to burst or to maximum design pressure, whichever occurs first. Six tests in helium and nine tests in hydrogen are recommended to be evenly distributed up to 1000bar/min pressure rise rate. After carrying out pressure corrections as outlined in the standard, the ratio of burst pressures at each test point are calculated. If the ratio of helium rupture pressure to hydrogen pressure is less than a certain ratio, than the selected material is considered as suitable for hydrogen service.

The second (method B) and third (method C) test methods in Part 4 relies on fracture mechanics principles and mainly based on BS EN ISO 7539 standard[104], which outlines stress corrosion testing procedures. Both methods require a fatigue pre-cracked compact tension C(T) specimen geometry.

Method B aims to determine the threshold stress intensity factor for hydrogen assisted cracking, KIH, by combination of applying a constant load for a certain period then incrementally increasing tensile load, which is different than the constant load approach as discussed in KD-10[96] previously. After a high purity test chamber is achieved, e.g. 99.9995% hydrogen, the test begins with applying a load that will generate a stress intensity factor at the crack tip that is significantly lower than the KIH value. The test specimen is subjected to this initial load for 20 minutes and any potential crack growth is monitored using the direct current potential (DCPD)

Funded by the European Union. Views and opinions expressed are however those of the author(s) only and do not necessarily reflect those of the European Union or [name of the granting authority]. Neither the European Union nor the granting authority can be held responsible for them.

method. If no potential drop is observed after 20 minutes, the test continues by increasing the applied load by a further 1MPa√m at the crack tip and then subjecting the test specimen to this new load for 20 minutes. This procedure of stepwise load increase and 20-minute hold is carried out until the test specimen failure. After conclusion of the test, KIH value is calculated as per the equation given in BS EN ISO 7539-6[105] using the load before the final step that caused failure. If the calculated is equal or higher than a certain empirical value based on material tensile strength, then the material can be accepted hydrogen service up to the test specimen thickness used during testing.

Method C is a constant displacement method that aims to investigate crack extension under application of a specific stress intensity factor at the crack tip for a certain amount of time. Although this method is similar to the approach presented in ASTM E1681[100], the techniques of applying a constant displacement load is different and according to the standard ISO 7539-6[105]. After a high purity test chamber is achieved, target stress intensity factor at the crack tip to be achieved by displacement loading is given depending on the material tensile strength, which is applied for at least 1,000 hours. Afterwards, the specimen is broken open and investigated under a scanning electron microscope. If the measured crack extension does not exceed 0.25mm, then the selected material qualifies for the hydrogen service. Alternatively, if the crack extension exceeded 0.25mm, but the calculated stress intensity factor is less than a certain empirical value based on material tensile strength, then the material is still deemed acceptable for hydrogen service.

In summary, pressure vessel standards require additional mechanical testing for vessels intended for hydrogen service. The philosophy of testing in BS EN ISO 11114[93] are geared towards material qualification, e.g. the dimensioning approach is unchanged, and the material of interest can be accepted or rejected for service depending on mechanical testing results in relevant hydrogen environment. In contrast, ASME KD-10 limits dimensioning options to fracture mechanics-based approaches in presence of hydrogen, and the mechanical testing is used to generate relevant material data to be used in fracture mechanics approaches.

4.7.3 Slow strain rate testing (SSRT)

SSRT is a screening type test that indicates hydrogen embrittlement of a material within a reasonable timeframe; the aim is to evaluate degradation in tensile strength and ductility due to hydrogen exposure with respect to mechanical properties obtained in an inert environment. SSRT is usually carried out using a smooth cylindrical test specimen under axial tension load inside a sealed chamber with the desired environment. However, different specimen types, e.g. notched, and test setups, e.g. bending load, can also be observed in practice.

The main body of standards ASTM G129[106] and BS EN ISO 7539-7[107] cover various corrosive environments including aquatic, nonaquatic, and gaseous service, whereas ASTM G142 [108] is dedicated for high pressure and/or high temperature hydrogen environment. Details of the test procedure along with recommendations on test specimen geometry and applied strain rate can be found in the referenced standards.

As can be inferred from the test name, the applied strain rate is slower compared to the conventional tensile tests as described in ASTM E8/E8M[109] or BS EN ISO 6892[110]. The aim is to accelerate the environmental influence on mechanical properties (if any), hence the service conditions might be quite different from the test conditions, which is why the “screening” remark was made in the beginning of this sub-section. In this regard, a typical sketch is shown in Figure 17.

Funded by the European Union. Views and opinions expressed are however those of the author(s) only and do not necessarily reflect those of the European Union or [name of the granting authority]. Neither the European Union nor the granting authority can be held responsible for them.

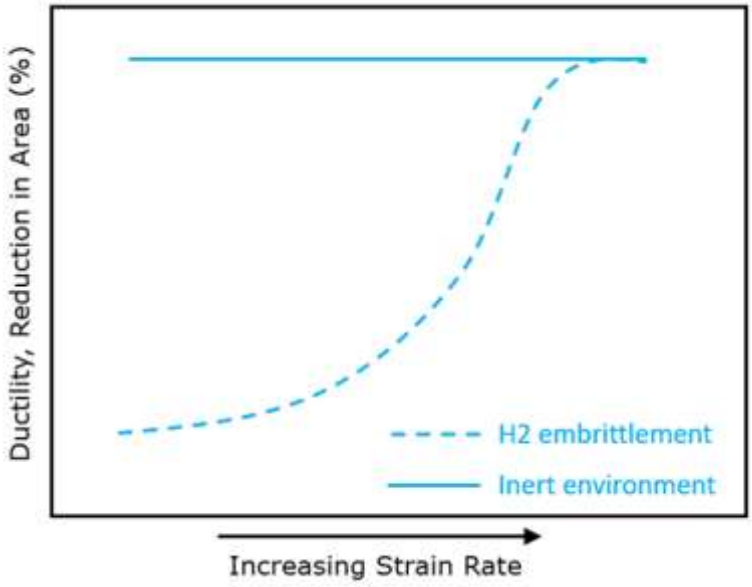

Figure 17: The influence of applied strain rate on ductility[111] *(ASTM, 2021)*

Figure 17 shows that as the applied strain rate is reduced, the ductility does not change in an inert environment, whereas it reduces monotonically in a hydrogen environment. In order to explore the environmental influence on mechanical properties, referenced standards target slow strain rates to simulate the behaviour shown in Figure 17. ASTM G142[108] suggests an initial 0.002mm/s ± %10 crosshead extension rate, which turns out to be ~7 x 10-5s-1 strain rate if the recommended test specimen geometry with 28.6mm gauge length is considered. Given that ASTM G129[106] and ISO 7539-7[107] cover a variety of environmental conditions, they suggest a wider range of initial applied strain rates from 10-3s-1 to 10-7s-1, and the selection is left to the user depending on the environment of interest.

As discussed in the beginning, mechanical properties obtained from SSRT tests are compared to mechanical properties in an inert environment; some researchers and standards suggest an index ratio based on this comparison, which allows rapidly ranking hydrogen embrittlement of various materials.

4.7.4 Fracture toughness testing in presence of hydrogen

The aim of fracture toughness testing in hydrogen environment is to determine a threshold value below which a crack does not propagate; this threshold value is often denoted by KIH. In contrast to SSRT, fracture toughness testing can be used in engineering critical assessments, but it is limited to crack propagation stage only since a pre-cracked test specimen is used. Constant load or constant displacement test methods can be used to determine KIH, which are covered by standards ASTM E1681[100]and BS EN ISO 7539-6[112]. Furthermore, rising load/displacement techniques have also become available[113,114], which provide faster results compared to constant load/displacement methods and could be more suitable approach to determine KIH for some materials[115].

In a constant load test, a pre-cracked test specimen is placed in a desired environment and then subjected to a constant load, which is denoted by Ki. After a certain period, sealed environmental chamber is opened and test specimen is investigated under high magnification microscopy to determine crack extension. If the crack extension is below a certain value, then applied initial value Ki qualifies as KIH. Despite the relatively easy test setup, test duration can be quite long, ranging from 1,000 hours to 10,000 hours as per ASTM E1681[100]. Furthermore, it is reported that as the applied Ki reduces, the crack incubation period increases[116]. Thus, the

Funded by the European Union. Views and opinions expressed are however those of the author(s) only and do not necessarily reflect those of the European Union or [name of the granting authority]. Neither the European Union nor the granting authority can be held responsible for them.

absence of any observable crack extension in a constant load test does not conclusively eliminate environmental crack growth, because the crack might be still in the incubation period.

Constant displacement test, on the other hand, is considered to be more robust method to establish KIH compared to a constant load test[116], since it can deal with the crack incubation problem by applying a high Ki in the beginning, and thus reduce the incubation period. In these tests, the pre-cracked test specimen is loaded to a selected crack mouth opening displacement (CMOD) by tensioning a bolt, noting that there are expressions available to relate CMOD to stress intensity factor, Ki. In this setup, the applied high Ki in the beginning will reduce as the crack grows, therefore after sufficiently long test duration, the crack will arrest once the Ki reach the threshold value KIH.

In "rising" fracture test methods, a sufficiently low loading or displacement rate is selected to allow hydrogen diffusion from environment to crack tip zone. The remainder of the test can be similar to usual resistance curve (R-curve) test, and the calculation of KIH is subjective to standard of interest but could be based on empirical formulations or the onset crack propagation. Similar to SSRT method, the selected initial loading rate can have a significant influence on the obtained fracture toughness values.

4.7.5 Fatigue endurance and fatigue crack growth testing in presence of hydrogen

As per authors' best knowledge, a dedicated fatigue testing standard in hydrogen environment is not available. Therefore, procedures developed for laboratory air tests are followed in practice using standardised test specimen geometries, e.g. ASTM E466[117] for fatigue endurance testing and ASTM E647[101] for fatigue crack growth rate testing.

As seen in literature[118], fatigue tests are realised by fitting a bespoke vessel in standard servo-hydraulic fatigue testing machines. The test specimen is mounted inside this bespoke vessel, which is subsequently purged and pressurised with the environment of interest. Given that the vessel will be sealed during testing, the standard load cell of the servo-hydraulic machine will be affected by seal friction. Therefore, a further second load cell is often needed inside the sealed vessel to apply desired loads.

Although fatigue endurance tests and the corresponding total life (S-N) approach for fatigue design are considered in the main body of pressure vessel standards, this approach is not allowed for fatigue assessment in presence of hydrogen, see[96]. Yet, fatigue endurance tests in hydrogen are common in literature and can provide valuable information as it characterises both crack initiation and crack propagation stages.

In contrast, fatigue crack growth rate test that characterise only the crack propagation stage is specified in some of the pressure vessel standards, see[96], thus it can be considered essential for engineering design. As discussed, environmental cracking is time dependent, hence the applied cyclic loading frequency and its shape can have a significant influence on fatigue crack growth. Given that the material testing standards such as ASTM E647[101] intended for inert environments, there is no guidance available for applied load frequency. Furthermore, parameters that are known to influence fatigue such as surface quality and stress ratio should also be considered in test specimen design and test specifications, if possible, match with the intended application. Finally, fatigue crack growth rate tests can be limited to increasing/decreasing ΔK tests to determine stage II crack propagation zone, i.e. Paris regime, given that the design criteria in reviewed pressure vessel standards require only this region without the threshold stress intensity factor value for fatigue crack propagation, ΔKth.

4.7.6 Evaluating performance of coatings against hydrogen embrittlement

Surface coatings, which separate the hydrogen environment from the structure, can provide physical barrier

Funded by the European Union. Views and opinions expressed are however those of the author(s) only and do not necessarily reflect those of the European Union or [name of the granting authority]. Neither the European Union nor the granting authority can be held responsible for them.

against hydrogen permeation inside the material. Although there are many dedicated standards are available to determine coating properties, e.g. adhesion strength ASTM C633[119], the protective performance of a surface coating is generally assessed using the material test standards described so far. In this approach, a control group, e.g. uncoated test specimens, and a test group, e.g. coated test specimens, are required. For example, in literature Yamabe et al.[120] evaluated the coating performance by measuring the hydrogen content gas chromatography-mass spectrometry (GC–MS), then Hwang et al.[80] evaluated PTFE coating performance using pre-charged samples and Charpy impact testing. Another example is Michler et al.[121] in which SSRT method was used to evaluate coating performance by comparing tests results of coated and uncoated samples.

Funded by the European Union. Views and opinions expressed are however those of the author(s) only and do not necessarily reflect those of the European Union or [name of the granting authority]. Neither the European Union nor the granting authority can be held responsible for them.

5 CONCLUSIONS

5.1 HYDROGEN EMBRITTLEMENT OF LIGHTWEIGHT ALLOYS

- Aluminium alloys and their weldments are immune to the deleterious effects of hydrogen embrittlement when exposed to pure dry hydrogen environments. Introduction of moisture into high pressure hydrogen gas environments can lead to hydrogen embrittlement.
- Aluminium alloys have very low hydrogen solid solution solubility under 1 ppm but increases to over few ppm levels in liquid phase thus leading to porosity upon solidification at high cooling rates.
- Hydrogen diffusion coefficient of pure aluminium was reported to be within the range of10^{-14} m^2s^{-1}
- Aluminium alloy solid solution strengthened grades (Al-Mg) with high magnesium content are susceptible to hydrogen environmental assisted cracking in moist and distilled water environments, especially when in the sensitized condition.
- Precipitation hardened aluminum alloys based on Zn-Mg (Cu) grades are highly susceptible to hydrogen environment assisted cracking in moist environments, down to relative humidity levels of 20%.
- Further research is required to establish the hydrogen performance of AM equivalent of 5xxx and 7xxx aluminium alloy grades.
- Magnesium alloys are not suitable for long term hydrogen storage applications due to the formation magnesium hydrides that will eventually lead to environmental assisted cracking.

5.2 waDED ALLOYS FOR HYDROGEN CRYOGENIC APPLICATIONS

- The literature review confirms aluminium alloys as promising structural material for cryogenic hydrogen storage tanks.
- The face centered cubic lattice structure of aluminium is responsible for very good mechanical properties at cryogenic conditions compared to bcc or hcp (magnesium) materials.
- The influence of waDED microstructure on cryogenic performance needs to be investigated.
- The influence of waDED microstructure on hydrogen embrittlement needs to be investigated.

5.3 COATINGS LITERATURE REVIEW

- From a literature review a lack of literature was available in terms of *coatings* + *aluminum alloy* + *corrosion protection* + *hydrogen storage applications.*
- D4.1 describes some scientific publications in terms of organic coatings: epoxy, PTFE and polyurethane coatings.
- According to the literature review, epoxy coatings are the most promising materials to prevent HE on aluminium alloys. Commercial products with an operating condition of cryogenic temperature (-196 ºC) and high corrosion resistance were found. Adhesion must be tested in lightweight metal alloys manufactured by waDED.

5.4 HYDROGEN TESTING METHODOLOGIES

- Both hydrogen and low temperatures can degrade mechanical properties individually, however, a pressure vessel design standard accounting the interplay between high pressure hydrogen and low temperatures for lightweight alloys is not available at the moment. Consequently, there is a need to develop a mechanical testing program for determining the potential influence of specific environmental conditions on selected lightweight alloys in this project.
- Given the need for developing a project specific mechanical testing program, this document provided a review of available pressure vessel design practices and material testing standards covering hydrogen service.
- Material testing standards for hydrogen service can be broadly divided into two categories: screening

Funded by the European Union. Views and opinions expressed are however those of the author(s) only and do not necessarily reflect those of the European Union or [name of the granting authority]. Neither the European Union nor the granting authority can be held responsible for them.

tests that allow ranking materials within a reasonable timeframe and fatigue & fracture tests that can be used in engineering calculations. Although international standards are available for both categories, the influence of hydrogen on mechanical properties is still an active research area and the test results might require expert judgement for interpretation. Finally, material testing in hydrogen environment requires specialised, purpose-built facilities that are not immediately available everywhere, and material testing can prolong many months to obtain sensible results given that environmental assisted cracking is a time dependent process.

Funded by the European Union. Views and opinions expressed are however those of the author(s) only and do not necessarily reflect those of the European Union or [name of the granting authority]. Neither the European Union nor the granting authority can be held responsible for them.

6 REFERENCES

(1) Lynch, S. Hydrogen Embrittlement Phenomena and Mechanisms. *Corrosion Reviews* **2012**, *30* (3–4). https://doi.org/10.1515/corrrev-2012-0502.

(2) W. H. Johnson. II. On Some Remarkable Changes Produced in Iron and Steel by the Action of Hydrogen and Acids. *Proceedings of the Royal Society of London* **1875**, *23* (156–163), 168–179. https://doi.org/10.1098/rspl.1874.0024.

(3) McFalls, T. The Effect of Hydrogen on Gas Porosity in Laser Powder Bed Fusion of AlSi10Mg - Master Thesis, University of Tennessee, USA, 2018.

(4) Lynch, S. Mechanistic and Fractographic Aspects of Stress Corrosion Cracking. *Corrosion Reviews* **2012**, *30* (3–4). https://doi.org/10.1515/corrrev-2012-0501.

(5) Omiyale, B. O.; Olugbade, T. O.; Abioye, T. E.; Farayibi, P. K. Wire Arc Additive Manufacturing of Aluminium Alloys for Aerospace and Automotive Applications: A Review. *Materials Science and Technology* **2022**, *38* (7), 391–408. https://doi.org/10.1080/02670836.2022.2045549.

(6) Ltd., TWI. *MOISTURE/HYDROGEN IN SHIELDING GAS OF GAS METAL ARC WELDS*. [Online] TWI Ltd. [Cited: 23 1 2023]. https://www.twi-global.com/ (accessed 2023-02-28).

(7) Scully, J. R.; Young, G. A.; Smith, S. W. Hydrogen Embrittlement of Aluminum and Aluminum-Based Alloys. In *Gaseous Hydrogen Embrittlement of Materials in Energy Technologies*; Elsevier, 2012; pp 707–768. https://doi.org/10.1533/9780857093899.3.707.

(8) Aboura, Y.; Garner, A. J.; Euesden, R.; Barrett, Z.; Engel, C.; Holroyd, N. J. H.; Prangnell, P. B.; Burnett, T. L. Understanding the Environmentally Assisted Cracking (EAC) Initiation and Propagation of New Generation 7xxx Alloys Using Slow Strain Rate Testing. *Corros Sci* **2022**, *199*, 110161. https://doi.org/10.1016/j.corsci.2022.110161.

(9) Schwarzenböck, E.; Ollivier, E.; Garner, A.; Cassell, A.; Hack, T.; Barrett, Z.; Engel, C.; Burnett, T. L.; Holroyd, N. J. H.; Robson, J. D.; Prangnell, P. B. Environmental Cracking Performance of New Generation Thick Plate 7000-T7x Series Alloys in Humid Air. *Corros Sci* **2020**, *171*, 108701. https://doi.org/10.1016/j.corsci.2020.108701.

(10) Skúlason, E.; Karlberg, G. S.; Rossmeisl, J.; Bligaard, T.; Greeley, J.; Jónsson, H.; Nørskov, J. K. Density Functional Theory Calculations for the Hydrogen Evolution Reaction in an Electrochemical Double Layer on the Pt(111) Electrode. *Phys. Chem. Chem. Phys.* **2007**, *9* (25), 3241–3250. https://doi.org/10.1039/B700099E.

(11) Campbell, J. E. *Effects of Hydrogen Gas on Metals at Ambient Temperature*; 1970.

(12) Speidel, M. O.; Hyatt, M. v. Stress-Corrosion Cracking of High-Strength Aluminum Alloys. In *Advances in Corrosion Science and Technology*; Springer US: Boston, MA, 1972; pp 115–335. https://doi.org/10.1007/978-1-4615-8255-7_3.

(13) Lorenz, P. M. *Effect of Pressurized Hydrogen upon Inconel 718 and 2219 Aluminum*; 1969.

(14) Holroyd, N. J. H.; Scamans, G. M. Stress Corrosion Cracking in Al-Zn-Mg-Cu Aluminum Alloys in Saline Environments. *Metallurgical and Materials Transactions A* **2013**, *44* (3), 1230–1253. https://doi.org/10.1007/s11661-012-1528-3.

Funded by the European Union. Views and opinions expressed are however those of the author(s) only and do not necessarily reflect those of the European Union or [name of the granting authority]. Neither the European Union nor the granting authority can be held responsible for them.

(15) Holroyd, N. J. H.; Scamans, G. M. Crack Propagation During Sustained-Load Cracking of Al-Zn-Mg-Cu Aluminum Alloys Exposed to Moist Air or Distilled Water. *Metallurgical and Materials Transactions A* **2011**, *42* (13), 3979–3998. https://doi.org/10.1007/s11661-011-0793-x.

(16) H.K. Birnbaum, C. B. F. Z. E. S. P. R. S. S. J. S. Lin. Hydrogen in Aluminum. *J Alloys Compd* **1997**, *253–254*.

(17) Ambat, R.; Dwarakadasa, E. S. Effect of Hydrogen in Aluminium and Aluminium Alloys: A Review. *Bulletin of Materials Science* **1996**, *19* (1), 103–114. https://doi.org/10.1007/BF02744792.

(18) Anyalebechi, P. N. Analysis and Thermodynamic Prediction of Hydrogen Solution in Solid and Liquid Multicomponent Aluminum Alloys. In *Essential Readings in Light Metals*; Springer International Publishing: Cham, 2016; pp 185–200. https://doi.org/10.1007/978-3-319-48228-6_23.

(19) WATSON, J. W.; MESHII, M. Hydrogen in Aluminum and Aluminum Alloys; 1989; pp 501–521. https://doi.org/10.1016/B978-0-12-341831-9.50023-1.

(20) Anyalebechi, P. Critical Review of Reported Values of Hydrogen Diffusion in Solid and Liquid Aluminum and Its Alloys. *TMS Light Metal* **2003**.

(21) Talbot, D. Effects of Hydrogen in Aluminium, Magnessium, Copper and Their Alloys. *International metallurgical reviews* **1975**, *20*.

(22) Holroyd, N. J. H.; Hardie, D. Strain-Rate Effects in the Environmentally Assisted Fracture of a Commercial High-Strength Aluminium Alloy (7049). *Corros Sci* **1981**, *21* (2), 129–144. https://doi.org/10.1016/0010-938X(81)90097-4.

(23) Gudla, V. C.; Storm, M.; Palmer, B. C.; Lewandowski, J. J.; Withers, P. J.; Holroyd, N. J. H.; Burnett, T. L. Environmentally Induced Crack (EIC) Initiation, Propagation, and Failure: A 3D in-Situ Time-Lapse Study of AA5083 H131. *Corros Sci* **2020**, *174*, 108834. https://doi.org/10.1016/j.corsci.2020.108834.

(24) Kappes, M.; Iannuzzi, M.; Carranza, R. M. Hydrogen Embrittlement of Magnesium and Magnesium Alloys: A Review. *J Electrochem Soc* **2013**, *160* (4), C168–C178. https://doi.org/10.1149/2.023304jes.

(25) Birnbaum, H. K. *Mechanisms of Hydrogen Related Fracture of Metals*; Houston, TX , 1990.

(26) Okamoto, H. H-Mg (Gydrogen-Magnesium). *Journal of Phase Equilibria* **2001**, *22* (5), 598.

(27) Zeng, K. Critical Assessment and Thermodynamic Modeling of the Mg–H System. *Int J Hydrogen Energy* **1999**, *24* (10), 989–1004. https://doi.org/10.1016/S0360-3199(98)00132-3.

(28) Nishimura, C.; Komaki, M.; Amano, M. Hydrogen Permeation through Magnesium. *J Alloys Compd* **1999**, *293–295*, 329–333. https://doi.org/10.1016/S0925-8388(99)00373-4.

(29) Atrens, A.; Winzer, N.; Song, G.; Dietzel, W.; Blawert, C. Stress Corrosion Cracking and Hydrogen Diffusion in Magnesium. *Adv Eng Mater* **2006**, *8* (8), 749–751. https://doi.org/10.1002/adem.200600050.

(30) Dietzel, W.; Pfuff, M.; Winzer, N. Testing and Mesoscale Modelling of Hydrogen Assisted Cracking of Magnesium. *Eng Fract Mech* **2010**, *77* (2), 257–263. https://doi.org/10.1016/j.engfracmech.2009.07.009.

(31) Zakroczymski, T. The Effect of Straining on the Transport of Hydrogen in Iron, Nickel, and Stainless Steel. *CORROSION* **1985**, *41* (8), 485–489. https://doi.org/10.5006/1.3583831.

Funded by the European Union. Views and opinions expressed are however those of the author(s) only and do not necessarily reflect those of the European Union or [name of the granting authority]. Neither the European Union nor the granting authority can be held responsible for them.

(32) Szklarska-Smialowska, Z.; Xia, Z. Hydrogen Trapping by Cold-Worked X-52 Steel. *Corros Sci* **1997**, *39* (12), 2171–2180. https://doi.org/10.1016/S0010-938X(97)00100-5.

(33) San-Martin, A.; Manchester, F. D. The H−Mg (Hydrogen-Magnesium) System. *Journal of Phase Equilibria* **1987**, *8* (5), 431–437. https://doi.org/10.1007/BF02893152.

(34) Krozer, A.; Kasemo, B. Equilibrium Hydrogen Uptake and Associated Kinetics for the Mg-H_2 System at Low Pressures. *Journal of Physics: Condensed Matter* **1989**, *1* (8), 1533–1538. https://doi.org/10.1088/0953-8984/1/8/017.

(35) Popovic, Z. D.; Piercy, G. R. Measurement of the Solubility of Hydrogen in Solid Magnesium. *Metallurgical Transactions A* **1975**, *6* (10), 1915–1917. https://doi.org/10.1007/BF02646856.

(36) Winzer, N.; Atrens, A.; Dietzel, W.; Song, G.; Kainer, K. U. Fractography of Stress Corrosion Cracking of Mg-Al Alloys. *Metallurgical and Materials Transactions A* **2008**, *39* (5), 1157–1173. https://doi.org/10.1007/s11661-008-9475-8.

(37) Winzer, N.; Atrens, A.; Dietzel, W.; Raja, V. S.; Song, G.; Kainer, K. U. Characterisation of Stress Corrosion Cracking (SCC) of Mg–Al Alloys. *Materials Science and Engineering: A* **2008**, *488* (1–2), 339–351. https://doi.org/10.1016/j.msea.2007.11.064.

(38) Lynch, S. P.; Trevena, P. Stress Corrosion Cracking and Liquid Metal Embrittlement in Pure Magnesium. *CORROSION* **1988**, *44* (2), 113–124. https://doi.org/10.5006/1.3583907.

(39) Chawla, N.; Chawla, K. K. *Metal Matrix Composites*; Springer New York: New York.

(40) Ou, Y.; Zhu, D.; Zhang, H.; Yao, Y.; Mobasher, B.; Huang, L. Mechanical Properties and Failure Characteristics of CFRP under Intermediate Strain Rates and Varying Temperatures. *Compos B Eng* **2016**, *95*, 123–136. https://doi.org/10.1016/j.compositesb.2016.03.085.

(41) Nishida, Y. *Introduction to Metal Matrix Composites*; Springer Tokyo: Tokyo.

(42) Society of Automotive Engineers. *Composite Materials Handbook. Volume 4, Metal Matrix Composites*.

(43) Chawla, K. K. *Composite Materials Science and Engineering Fourth Edition*.

(44) Graziano, R. P.; Candidato, U.; Fernandez, V. G. *Optimization of the Gas Pressure Infiltration Process for Aluminium Matrix Composites Manufacturing*; 2018.

(45) Shirvanimoghaddam, K.; Hamim, S. U.; Karbalaei Akbari, M.; Fakhrhoseini, S. M.; Khayyam, H.; Pakseresht, A. H.; Ghasali, E.; Zabet, M.; Munir, K. S.; Jia, S.; Davim, J. P.; Naebe, M. Carbon Fiber Reinforced Metal Matrix Composites: Fabrication Processes and Properties. *Composites Part A: Applied Science and Manufacturing*. Elsevier Ltd January 1, 2017, pp 70–96. https://doi.org/10.1016/j.compositesa.2016.10.032.

(46) Zhang, J.; Liu, S.; Zhang, Y.; Dong, Y.; Lu, Y.; Li, T. Fabrication of Woven Carbon Fibers Reinforced Al-Mg (95-5 Wt%) Matrix Composites by an Electromagnetic Casting Process. *J Mater Process Technol* **2015**, *226*, 78–84. https://doi.org/10.1016/j.jmatprotec.2015.06.040.

(47) Gordon, B. Metal Prepreg Technology Update; SAMPE: Long Beach, CA., 2005.

(48) Gordon, B. Metal Prepreg Filament Winding. *SAMPE Journal* **2006**, *42* (5).

Funded by the European Union. Views and opinions expressed are however those of the author(s) only and do not necessarily reflect those of the European Union or [name of the granting authority]. Neither the European Union nor the granting authority can be held responsible for them.

(49) Conrad, G.; Watt, R.; Kyle-Henney, S. *An Investigation of the Use of Metal Matrix Composites for Pressure Vessels Engineering Doctorate in Micro-and Nano-Materials and Technologies*; 2017.

(50) Wang, H.; Jiang, W.; Ouyang, J.; Kovacevic, R. Rapid Prototyping of 4043 Al-Alloy Parts by VP-GTAW. *J Mater Process Technol* **2004**, *148* (1), 93–102. https://doi.org/10.1016/j.jmatprotec.2004.01.058.

(51) Klein, T.; Graf, G.; Staron, P.; Stark, A.; Clemens, H.; Spoerk-Erdely, P. Microstructure Evolution Induced by the Intrinsic Heat Treatment Occurring during Wire-Arc Additive Manufacturing of an Al-Mg-Zn-Cu Crossover Alloy. *Mater Lett* **2021**, *303*. https://doi.org/10.1016/j.matlet.2021.130500.

(52) Klein, T.; Schnall, M. Control of Macro-/Microstructure and Mechanical Properties of a Wire-Arc Additive Manufactured Aluminum Alloy. *International Journal of Advanced Manufacturing Technology* **2020**, *108* (1–2), 235–244. https://doi.org/10.1007/s00170-020-05396-6.

(53) Klein, T.; Arnoldt, A.; Schnall, M.; Gneiger, S. Microstructure Formation and Mechanical Properties of a Wire-Arc Additive Manufactured Magnesium Alloy. *JOM* **2021**, *73* (4), 1126–1134. https://doi.org/10.1007/s11837-021-04567-4.

(54) Gneiger, S.; Österreicher, J. A.; Arnoldt, A. R.; Birgmann, A.; Fehlbier, M. Development of a High Strength Magnesium Alloy for Wire Arc Additive Manufacturing. *Metals (Basel)* **2020**, *10* (6), 1–14. https://doi.org/10.3390/met10060778.

(55) Kammer, C. *Aluminium Taschenbuch 3: Weiterverarbeitung und Anwendung*; Beuth Verlag, 2014.

(56) Wu, B.; Pan, Z.; Ding, D.; Cuiuri, D.; Li, H.; Xu, J.; Norrish, J. A Review of the Wire Arc Additive Manufacturing of Metals: Properties, Defects and Quality Improvement. *Journal of Manufacturing Processes*. Elsevier Ltd October 1, 2018, pp 127–139. https://doi.org/10.1016/j.jmapro.2018.08.001.

(57) Cong, B.; Ding, J.; Williams, S. Effect of Arc Mode in Cold Metal Transfer Process on Porosity of Additively Manufactured Al-6.3%Cu Alloy. *International Journal of Advanced Manufacturing Technology* **2015**, *76* (9–12), 1593–1606. https://doi.org/10.1007/s00170-014-6346-x.

(58) Williams, S. W.; Martina, F.; Addison, A. C.; Ding, J.; Pardal, G.; Colegrove, P. Wire + Arc Additive Manufacturing. *Materials Science and Technology (United Kingdom)* **2016**, *32* (7), 641–647. https://doi.org/10.1179/1743284715Y.0000000073.

(59) Izumi, T.; Itoh, G. Thermal Desorption Spectroscopy Study on the Hydrogen Trapping States in a Pure Aluminum. *Mater Trans* **2011**, *52* (2), 130–134. https://doi.org/10.2320/matertrans.L-M2010825.

(60) Safyari, M.; Moshtaghi, M.; Kuramoto, S. On the Role of Traps in the Microstructural Control of Environmental Hydrogen Embrittlement of a 7xxx Series Aluminum Alloy. *J Alloys Compd* **2021**, *855*, 157300. https://doi.org/10.1016/j.jallcom.2020.157300.

(61) Safyari, M.; Moshtaghi, M.; Hojo, T.; Akiyama, E. Mechanisms of Hydrogen Embrittlement in High-Strength Aluminum Alloys Containing Coherent or Incoherent Dispersoids. *Corros Sci* **2022**, *194*. https://doi.org/10.1016/j.corsci.2021.109895.

(62) Hurlich, A. Low Temperature Metals. *Chemical Engineering* **1963**, 311–325.

(63) Gottstein, G. *Materialwissenschaft Und Werkstofftechnik*; Springer Berlin Heidelberg: Berlin, Heidelberg, 2014. https://doi.org/10.1007/978-3-642-36603-1.

(64) Ui, G. G.; Sang, H. L.; Won, J. N. The Evolution of Microstructure and Mechanical Properties of a 5052

Funded by the European Union. Views and opinions expressed are however those of the author(s) only and do not necessarily reflect those of the European Union or [name of the granting authority]. Neither the European Union nor the granting authority can be held responsible for them.

Aluminium Alloy by the Application of Cryogenic Rolling and Warm Rolling. In *Materials Transactions*; 2009; Vol. 50, pp 82–86. https://doi.org/10.2320/matertrans.MD200801.

(65) Sonia, P.; Verma, V.; Saxena, K. K.; Kishore, N.; Rana, R. S. Effect of Cryogenic Treatment on Mechanical Properties and Microstructure of Aluminium 6082 Alloy. In *Materials Today: Proceedings*; Elsevier Ltd, 2019; Vol. 26, pp 2248–2253. https://doi.org/10.1016/j.matpr.2020.02.488.

(66) Jordan, J. *Ductile to brittle transitions in materials*.

(67) E28 Commitee. *Designation: E8/E8M − 13a Standard Test Methods for Tension Testing of Metallic Materials 1*; 2019. https://doi.org/10.1520/E0008_E0008M-13A.

(68) ASTM-B07.05. *ASTM-B557-15-Standard-Test-Methods-for-Tension-Testing-Wrought-and-Cast-Aluminum-and-Magnesium-Alloy-Products*; 2016. https://doi.org/10.1520/B0557-15.

(69) Kaufman, J. G. (John G. *Properties of Aluminum Alloys : Tensile, Creep, and Fatigue Data at High and Low Temperatures*; ASM International, 1999.

(70) Jacqueline I. Kroschwitz. Concise Encyclopedia of Polymer Science and Engineering. *Wiley-Interscience*; 1990; pp 344–1167.

(71) Khare, A.; Dwivedi, S. K.; Vishwakarma, M.; Ahmed, S. Experimental Investigation of Hydrogen Embrittlement during Coating Process and Effect on Mechanical Properties of High Strength Steel Used for Fasteners. *Mater Today Proc* **2018**, *5* (9), 18707–18715. https://doi.org/10.1016/j.matpr.2018.06.217.

(72) Niermann, D. Adhesive Bonding of Titanium. *Berichtsband - Deutsche Forschungsgesellschaft fuer Oberflaechenbehandlung* **2004**, *57*, 80–86.

(73) JOTUN. *TDS Epoxy HR*. https://www.jotun.com/Datasheets/Download?url=%2FTDS%2FTDS__1505__Epoxy%20HR__Euk__GB.pdf (accessed 2022-11-14).

(74) JOTUN. *TDS Jotatemp 250*. https://jotundatasheetsprod.blob.core.windows.net/tds/TDS%C2%A432222%C2%A4Jotatemp%20250%C2%A4Euk%C2%A4GB.pdf (accessed 2022-11-09).

(75) JOTUN. *TDS Jotatemp 1000*. https://jotundatasheetsprod.blob.core.windows.net/tds/TDS%C2%A448342%C2%A4Jotatemp%201000%C2%A4Euk%C2%A4GB.pdf (accessed 2022-11-09).

(76) CARBOLINE. *Thermaline ® 440 PRODUCT DATA SHEET SELECTION & SPECIFICATION DATA Generic Type Modified Epoxy Phenolic*; 2021. https://msds.carboline.com/servlet/FeedFile/11/prod/8578/PDS%3A%7BPC%3A8578%3BMID%3A1%3BLID%3A1%7D/Thermaline_440_PDS.pdf (accessed 2022-11-09).

(77) HEMPEL. *TDS Hempaprime_CUI_275*. https://www.hempel.com/-/media/Files/Global/PDF/Products-and-Brands/Hempaprime/Hempaprime-CUI-275-Leaflet.pdf (accessed 2022-11-09).

(78) PPG. *Aerocron™ 2100 TECHNICAL DATA SHEET Product Description*. https://www.ppgaerospace.com/Value/Innovation/Aerocron.aspx (accessed 2022-11-09).

(79) Wang, Z.; Wang, Y.; Afshan, S.; Hjalmarsson, J. A Review of Metallic Tanks for H2 Storage with a View

to Application in Future Green Shipping. *Int J Hydrogen Energy* **2021**, *46* (9), 6151–6179. https://doi.org/10.1016/j.ijhydene.2020.11.168.

(80) Hwang, J.-S.; Kim, J.-H.; Kim, S.-K.; Lee, J.-M. Effect of PTFE Coating on Enhancing Hydrogen Embrittlement Resistance of Stainless Steel 304 for Liquefied Hydrogen Storage System Application. *Int J Hydrogen Energy* **2020**, *45* (15), 9149–9161. https://doi.org/10.1016/j.ijhydene.2020.01.104.

(81) Ngene, P.; Westerwaal, R. J.; Sachdeva, S.; Haije, W.; de Smet, L. C. P. M.; Dam, B. Polymer-Induced Surface Modifications of Pd-Based Thin Films Leading to Improved Kinetics in Hydrogen Sensing and Energy Storage Applications. *Angewandte Chemie International Edition* **2014**, *53* (45), 12081–12085. https://doi.org/10.1002/anie.201406911.

(82) Narain, S. Cryogenic Testing of Protective Coating Systems for a Liquefied Natural Gas Project. *Mater Perform* **1998**, *37* (3), 28–32.

(83) Kumar, K. B. S. Application of Organic Protective Coatings in the Petrochemical Industry - a Few Case Histories. *Proc. - Semin. Polym. Surf. Coat.: Recent Dev.* **1982**, *Conference*, 90–91.

(84) Chen, Y.; Zhao, S.; Ma, H.; Wang, H.; Hua, L.; Fu, S. Analysis of Hydrogen Embrittlement on Aluminum Alloys for Vehicle-Mounted Hydrogen Storage Tanks: A Review. *Metals (Basel)* **2021**, *11* (8), 1303. https://doi.org/10.3390/met11081303.

(85) Dey, S.; Chattoraj, I. Interaction of Strain Rate and Hydrogen Input on the Embrittlement of 7075 T6 Aluminum Alloy. *Materials Science and Engineering: A* **2016**, *661*, 168–178. https://doi.org/10.1016/j.msea.2016.03.010.

(86) Barthélémy, H. Hydrogen Storage – Industrial Prospectives. *Int J Hydrogen Energy* **2012**, *37* (22), 17364–17372. https://doi.org/10.1016/j.ijhydene.2012.04.121.

(87) ANSI/CSA. ANSI/CSA CHMC 1-2014 (R2018) Test Methods for Evaluating Material Compatibility in Compressed Hydrogen Applications - Metals. CSA Group 2014.

(88) CGA. H-3: Standard for Cryogenic Hydrogen Storage. Compressed Gas Assocation, Inc. 2019.

(89) BSI. BS ISO 13985:2006 Liquid Hydrogen. Land Vehicle Fuel Tanks. BSI 2006.

(90) BSI. BS EN 13458-2:2002 Cryogenic Vessels. Static Vacuum Insulated Vessels. Design, Fabrication, Inspection and Testing. BSI 2002.

(91) BSI. BS EN 14197-1:2003 Cryogenic Vessels. Static Non-Vacuum Insulated Vessels Fundamental Requirements. BSI 2003.

(92) BSI. ISO 20421-1:2019 Cryogenic Vessels — Large Transportable Vacuum-Insulated Vessels — Part 1: Design, Fabrication, Inspection and Testing. British Standards Institute (BSI): London June 2019, pp 0–125.

(93) BSI. BS EN ISO 11114-1:2020 Gas Cylinders. Compatibility of Cylinder and Valve Materials with Gas Contents - Metallic Materials. BSI 2020.

(94) BSI. BS EN 1252-1:1998 Cryogenic Vessels. Materials - Toughness Requirements for Temperatures below -80°C. BSI 1998.

(95) BSI. BS EN 13445-8:2021 Unfired Pressure Vessels Additional Requirements for Pressure Vessels of Aluminium and Aluminium Alloys. BSI 2021.

Funded by the European Union. Views and opinions expressed are however those of the author(s) only and do not necessarily reflect those of the European Union or [name of the granting authority]. Neither the European Union nor the granting authority can be held responsible for them.

(96) ASME. BPVC-VIII-3 BPVC Section VIII-Rules for Construction of Pressure Vessels Division 3-Alternative Rules for Construction of High Pressure Vessels. ASME 2021.

(97) Wei, H. L.; Bhadeshia, H. K. D. H.; David, S. A.; DebRoy, T. Harnessing the Scientific Synergy of Welding and Additive Manufacturing. *Science and Technology of Welding and Joining* **2019**, *24* (5), 361–366. https://doi.org/10.1080/13621718.2019.1615189.

(98) Oliveira, J. P.; Santos, T. G.; Miranda, R. M. Revisiting Fundamental Welding Concepts to Improve Additive Manufacturing: From Theory to Practice. *Prog Mater Sci* **2020**, *107*, 100590. https://doi.org/10.1016/j.pmatsci.2019.100590.

(99) ISO. ISO/TR 15916:2015 Basic Considerations for the Safety of Hydrogen Systems. ISO 2015.

(100) ASTM. ASTM E1681-03 Standard Test Method For Determining A Threshold Stress Intensity Factor For Environment-Assisted Cracking Of Metallic Materials. ASTM 2020.

(101) ASTM. ASTM E647-15 Standard Test Method For Measurement Of Fatigue Crack Growth Rates. ASTM International.

(102) ASTM. E399 - 05 Standard Test Method for Linear-Elastic Plane-Strain Fracture Toughness K_{IC} of Metallic Materials. ASTM 2017.

(103) BSI. BS EN ISO 7866:2012+A1:2020 Gas Cylinders. Refillable Seamless Aluminium Alloy Gas Cylinders. Design, Construction and Testing. BSI 2012.

(104) ISO. ISO 7539-1:2012 Corrosion of Metals and Alloys — Stress Corrosion Testing — Part 1: General Guidance on Testing Procedures. ISO 2012.

(105) BSI. ISO 7539-6:2018 Corrosion of Metals and Alloys — Stress Corrosion Testing — Part 6: Preparation and Use of Precracked Specimens for Tests under Constant Load or Constant Displacement. BSI 2018.

(106) ASTM. ASTM G129 Standard Practice for Slow Strain Rate Testing to Evaluate the Susceptibility of Metallic Materials to Environmentally Assisted Cracking. ASTM 2021.

(107) BSI. BS EN ISO 7539-7:2005 Corrosion of Metals and Alloys. Stress Corrosion Testing - Method for Slow Strain Rate Testing. BSI 2005.

(108) ASTM. ASTM G142-98 Standard Test Method for Determination of Susceptibility of Metals to Embrittlement in Hydrogen Containing Environments at High Pressure, High Temperature, or Both. ASTM 2022.

(109) ASTM. E8/E8M - 21 Standard Test Methods for Tension Testing of Metallic Materials. ASTM 2022.

(110) ISO. ISO 6892-1:2020 Metallic Materials - Tensile Testing - Part 1: Method of Test at Room Temperature (ISO 6892-1:2019). *2020*. ISO.

(111) Henthorne, M. The Slow Strain Rate Stress Corrosion Cracking Test—A 50 Year Retrospective. *CORROSION* **2016**, *72* (12), 1488–1518. https://doi.org/10.5006/2137.

(112) ISO. ISO 7539-6:2011 Corrosion of Metals and Alloys — Stress Corrosion Testing — Part 6: Preparation and Use of Precracked Specimens for Tests under Constant Load or Constant Displacement. ISO 2011.

Funded by the European Union. Views and opinions expressed are however those of the author(s) only and do not necessarily reflect those of the European Union or [name of the granting authority]. Neither the European Union nor the granting authority can be held responsible for them.

(113) ASTM International. ASTM F1624-12 Standard Test Method for Measurement of Hydrogen Embrittlement Threshold in Steel by the Incremental Step Loading Technique. ASTM International: West Conshohocken, PA 19428-2959. United States November 1, 2018, pp 0–12.

(114) BSI. EN ISO 7539-9:2021 Corrosion of Metals and Alloys - Stress Corrosion Testing - Part 9: Preparation and Use of Pre-Cracked Specimens for Tests under Rising Load or Rising Displacement . BSI 2021.

(115) Kevin A. Nibur, B. P. S. C. S. M. J. W. F. I. M. D. P. S. G. A. H. *Measurement and Interpretation of Threshold Stress Intensity Factors for Steels in High-Pressure Hydrogen Gas*; Albuquerque, New Mexico 87185 and Livermore, California 94550, 2010.

(116) Anderson, T. L. *Fracture Mechanics*; CRC Press, 2005. https://doi.org/10.1201/9781315370293.

(117) ASTM. ASTM E466-21 Standard Practice For Conducting Force Controlled Constant Amplitude Axial Fatigue Tests Of Metallic Materials. ASTM International 2021.

(118) Somerday, B. P.; Campbell, J. A.; Lee, K. L.; Ronevich, J. A.; San Marchi, C. Enhancing Safety of Hydrogen Containment Components through Materials Testing under In-Service Conditions. *Int J Hydrogen Energy* **2017**, *42* (11), 7314–7321. https://doi.org/10.1016/j.ijhydene.2016.04.189.

(119) ASTM. ASTM C633-13 Standard Test Method For Adhesion Or Cohesion Strength Of Thermal Spray Coatings. ASTM International 2021.

(120) Yamabe, J.; Matsuoka, S.; Murakami, Y. Surface Coating with a High Resistance to Hydrogen Entry under High-Pressure Hydrogen-Gas Environment. *Int J Hydrogen Energy* **2013**, *38* (24), 10141–10154. https://doi.org/10.1016/j.ijhydene.2013.05.152.

(121) Michler, T.; Naumann, J. Coatings to Reduce Hydrogen Environment Embrittlement of 304 Austenitic Stainless Steel. *Surf Coat Technol* **2009**, *203* (13), 1819–1828. https://doi.org/10.1016/j.surfcoat.2009.01.013.

Funded by the European Union. Views and opinions expressed are however those of the author(s) only and do not necessarily reflect those of the European Union or [name of the granting authority]. Neither the European Union nor the granting authority can be held responsible for them.